Physics – Uspekhi **65** (4) 379 – 405 (2022)

REVIEWS OF TOPICAL PROBLEMS PACS numbers: **26.40.+r,** 96.50.Vg, 98.70.Sa

Particle acceleration in space: a universal mechanism?

M I Panasyuk, L I Miroshnichenko

DOI: https://doi.org/10.3367/UFNe.2021.07.039022

Contents

Abstract. Experimental evidence in favor of or against the existence of a universal mechanism for the acceleration of charged particles in the Universe is analyzed from the modern standpoint. We adopt a purely phenomenological approach to this very intricate problem, discussing spatial scales that range from the magnetospheres of Earth and other planets of the Solar System to the Sun's atmosphere, the heliosphere, supernovae, and extragalactic objects responsible for the generation of ultra-high-energy cosmic rays. We demonstrate a great variety of acceleration mechanisms operating in the Universe. However, data on the nuclear composition of accelerated particles obtained in numerous experiments may be indicative of a global nature of the Fermi-type stochastic acceleration mechanism inherent in various astrophysical objects. This mechanism may well be dominant over others, but a number of experimental observations are nevertheless inconsistent with that idea. It is possible that a hierarchy of accelerating mechanisms operates in some space objects, with preliminary acceleration by one mechanism followed by other mechanisms, acting sequentially or alternatively. We therefore discuss all currently available data for and against the global 'presence' of a Fermi-type acceleration mechanism.

Keywords: cosmic rays, acceleration sources and mechanisms, shock waves in space, plasma physics, composition, spectrum, anisotropy, new physics of nuclear interactions

M I Panasyuk [(1)], **L I Miroshnichenko** [(1, 2, *)]
[(1)] Skobeltsyn Institute of Nuclear Physics,
Lomonosov Moscow State University,
Leninskie gory 1, str. 2, 119234 Moscow, Russian Federation
[(2)] N V Pushkov Institute of Terrestrial Magnetism,
Ionosphere and Radio Wave Propagation,
Russian Academy of Sciences,
Kaluzhskoe shosse 4, 108840 Troitsk, Moscow, Russian Federation
E-mail: [(*)] leonty@izmiran.ru

Received 5 November 2020, revised 14 July 2021
Uspekhi Fizicheskikh Nauk **192** (4) 413 – 442 (2022)
Translated by S Alekseev

1. Introduction

The question of the origin of cosmic rays (CRs) arose almost immediately after their discovery in 1912 (see, e.g., [1–3]). Soon after physicists realized the extraterrestrial origin of

CRs, the question about their acceleration mechanism(s) arose. The American physicist W F G Swann is universally credited for having been the first who, back in 1933, noted the possibility of accelerating charged particles (electrons) to significant (relativistic) energies in space conditions (in the atmospheres of stars) [4]. Swann proposed an acceleration mechanism in which energies of relativistic CRs (electrons) can be attained under the action of the electromagnetic induction associated with alternating magnetic fields of stars. This later became known as the *betatron* mechanism.

Only nine years later, in 1942, ground-based CR observations first allowed reliably detecting solar energetic particles (SEPs) — relativistic protons from the Sun [5] (solar cosmic rays). This happened after a powerful solar flare on February 28, 1942. The fact that the particles were generated precisely by the Sun was not immediately appreciated, however. It took several more similar occasions for the discoverer himself [6] and then other researchers [7–9] to convince themselves that relativistic particles had indeed come from the Sun. After the registration of the fourth increase in the SEP flux on Earth's surface (November 19, 1949), the connection between the observed relativistic particles and solar flares became an indisputable fact, which then laid the foundation for a new respectable scientific concept (see, e.g., [10] for the details). This provided direct confirmation of the hypothesis [4] that charged particles can accelerate in stellar atmospheres. More than 25 years later, the same author [11] extended his ideas and expanded the capabilities of the originally proposed model. As regards galactic cosmic rays (GCRs), their nature actually remained unclear until the late 1940s.

Meanwhile, back in 1934, the authors of [12] expressed the idea that so-called novae and supernovae could be sources of GCRs. How fruitful this hypothesis turned out to be can be judged by the incessant flow of publications related to the theory of particle acceleration in supernova explosions or to experiments aimed at confirming this hypothesis.

Substantial progress on the problem of the origin of GCRs was made in 1949 by Fermi [13] (who subsequently refined his model; see [14]). He proposed a *stochastic* acceleration mechanism, which was radically different from the betatron one. According to [13, 14], GCRs originate and accelerate mainly in the interstellar medium. The main acceleration is caused by the direct interaction of particles with wandering magnetic fields (magnetic clouds) that fill the interstellar space. Since then, models of Fermi-type acceleration in various astrophysical sources have been the subject of numerous thorough studies as well as many discussions and disputes.

Several decades later, it became clear, however, that neither the betatron effect nor the Fermi mechanism was sufficient for describing the data accumulated in the observations of accelerated particles coming from various celestial objects. Due to the evident, and very significant, diversity of conditions in different regions of the Universe, the acceleration processes also turned out to be very numerous and varied. This is evidenced, in particular, by the data provided in monographs [15–19] and reviews [20, 21]. We note several important theoretical reviews of the problem, e.g., [22] (magnetic reconnection in astrophysics), [23] (acceleration mechanisms in space), and [24] (critical issues of SEP acceleration). Some special issues in the study of SEPs are considered in [25–27]. Books [28, 29] and papers [30–37] published in *Physics–Uspekhi* are devoted to topical problems of astrophysics and cosmic rays. The question of CR acceleration long ago branched off from the problem of the origin of high-energy particles observed near Earth and is part of a more general problem of charged particle acceleration in space (see, e.g., [17–19, 22, 23]). Acceleration is apparently omnipresent wherever electric fields exist, irrespective of their nature.

In view of the obvious physical diversity of the acceleration mechanisms, several topical questions are in order: (1) is a *universal* acceleration mechanism possible in space? (2) is there a main (i.e., *dominant*) acceleration mechanism in space? (3) is there a *hierarchy* of various mechanisms in astrophysical objects (and in astrophysics in general)? We address these questions at the level of their present-day understanding.

In this review, we attempt to answer the two first questions at least. For this, we first consider the *observational* pro et contra arguments from the standpoint of the possible existence of a universal (or at least *dominant*) mechanism of charged particle acceleration in the Universe. In doing so, we systematically proceed from Earth's magnetosphere to the Sun's atmosphere, through interplanetary space to the boundaries of the heliosphere, and to other stars, especially bursting supernovae, and further on to extragalactic sources of ultrahigh-energy cosmic rays (UHECRs) with energy $E > 3 \times 10^{18}$ eV.

Several important methodological remarks are in order. Starting the analysis (interpretation) of any process (phenomenon), any researcher typically envisages a presumed mental (phenomenological) picture of the phenomenon or even assumes some theoretical model. Relying primarily on observational data, we of course try to avoid any *a priori* ideas as much as possible. Our main focus is on observational data obtained for various regions of space, whenever possible, regardless of the models of one CR source or another. At the same time, we are aware that experimental results are always characterized by uncertainty due to both systematic (model) errors and an insufficiently high statistical accuracy of measurements. It is clear that, as the particle energies increase (with a decrease in the statistics of measurements), the quality of information deteriorates. The problem of model dependence of the results still exists, especially for UHECRs (see Section 9). We are also aware that it is impossible to fully reflect the current state of this rapidly developing field of cosmophysics. Particle acceleration in cosmic conditions is a very complex and multifaceted problem, and we are aware of the shortcomings of the phenomenological approach. We try to compensate for these shortcomings, at least partially, by selecting illustrations and a system of references to the original and/or review articles and monographs.

2. Cosmic rays near Earth

Before addressing problems related to the acceleration of particles in space, we present several important facts of a general astrophysical nature that are relevant to CRs. We first note that the mass composition, energy spectrum, and anisotropy of CRs, despite the inevitable statistical uncertainty of these parameters, are of crucial importance in verifying acceleration models.

2.1 Elemental composition of cosmic rays

In Fig. 1, we show the mean abundance of elements (atomic nuclei) in galactic and solar CRs. As we can see, GCRs in general contain very few high-energy heavy charged particles;

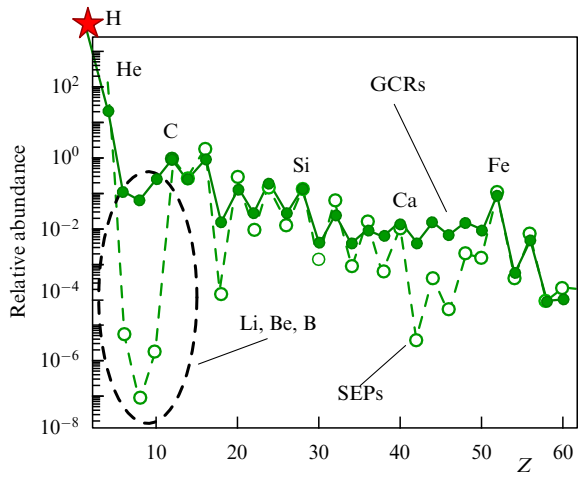

Figure 1. Mean abundance of elements (atomic nuclei) in GCRs and SEPs [29]. Carbon C content in GCRs is assumed to be 1.0.

for example, the Fe/H ratio is only $\sim 10^{-4}$–10^{-5} [29]. The SEP composition is not identical to that of GCRs. In SEP events, the content of high-energy heavy charged particles has features of its own. The difference is primarily determined by the absence of the light nuclei of Li, Be, and B in SEPs. In the composition of GCRs, these nuclei are obviously of secondary origin: they are produced in the process of fragmentation of heavier CR nuclei during their propagation through the interstellar medium. This fact is used, in particular, to obtain constraints on the GCR propagation models (see, e.g., [38, 39]). When particles pass from the Sun to Earth, these elements simply do not have time to be produced in nuclear reactions.

According to the content of Li, Be, and B nuclei that form as a result of the interaction of CRs with atoms of the interstellar medium, we can determine one more important characteristic: the wandering time t of CRs in the interstellar medium (their 'lifetime,' or 'age,' before reaching Earth). The amount of substance X through which CRs pass while wandering in the interstellar medium is approximately 5–10 g cm^{-2}. The age t and the value of X are related as $X \approx \rho v t$, where ρ is the mean density of the interstellar medium ($\sim 10^{-24}$ g cm^{-3}) and v is particle speed. For ultrarelativistic CRs, it is usually assumed that v is practically equal to the speed of light c, and hence t is about 3×10^8 years. The lifetime is determined either by the escape of CRs from the Galaxy and its halo or by their absorption as a result of inelastic interactions with the interstellar medium.

High-energy heavy charged particles are commonly referred to as HZE (the symbols standing for high (H), the atomic number (Z), and the particle energy (E)). HZE ions are high-energy GCR nuclei with a charge greater than +2: they include the nuclei of all elements heavier than hydrogen and helium. Despite the low abundance of HZE particles, their acceleration in various regions of outer space is of great interest, including in the question of the origin of UHECRs (see Sections 6 and 7). The HZE data are of particular interest in applications to problems of protecting astronauts and spacecraft (SCs) electronics from radiation, for radiobiology, for the theory of the origin of life and the evolution of Earth's biosphere, as well as for searching for life on other planets (see, e.g., [28, 29, 40–43]).

During solar flares, certain amounts of deuterium (D, or ^{2}H, a stable isotope of hydrogen), radioactive tritium ^{3}H, and several other radioactive isotopes of various elements are produced. It is generally accepted that the cosmic abundance of elements such as ^{2}H, ^{3}He, ^{4}He, and Li is the result of nuclear reactions in the first three minutes of the evolution of the universe. Important conclusions are hence drawn about the parameters of the Universe and its evolution.

2.2 Energy spectrum

In Fig. 2, we show the differential energy spectrum of 'all' CR particles, without dividing them into individual components. At energies above 10^{10}–10^{11} eV, the spectrum slope corresponds to the power law $\sim E^{-2.7}$. For even higher energies, the spectrum changes: the exponent increases in absolute value to 3.2 in the region of the so-called knee ($\geqslant 10^{15}$ eV). At energies $\geqslant 10^{10}$–10^{11} eV, particle fluxes are very stable, and in the energy range below this boundary, they experience strong variations under the influence of solar activity. The maximum recorded energy in the 'foot' area is 3×10^{20} eV.

The arrows in Fig. 2 show the main 'structural' features of the spectrum: the region of solar modulation (the influence of solar activity); the anomalous CR component; the 'knee' in the spectrum at $E \geqslant 10^{15}$ eV; and the 'foot' (or 'ankle') in the region of ultrahigh energies ($E \geqslant 10^{17}$ eV). In the energy range of $\sim 10^5$–10^9 eV, the so-called anomalous component of CRs (anomalous cosmic rays, ACRs) is observed.

For our presentation in what follows, Hillas diagrams [44] turn out to be quite useful. Such a diagram (Fig. 3) demonstrates the capabilities of various astrophysical objects as particle accelerators, albeit within the selected model of a shock wave (SW) that moves at a speed V_{sh} and accelerates particles via a Fermi-type mechanism. The maximum energy in model [44] is given by $E_{max} = \beta ZeBL$, where $\beta = V_{sh}/c$, c is the speed of light, Ze is the particle charge, B is the characteristic strength of the magnetic field of a given object, and L is/are its characteristic size.

The solid lines in Fig. 3 show estimates of the size L (expressed in parsecs) and the magnetic field strength B (in

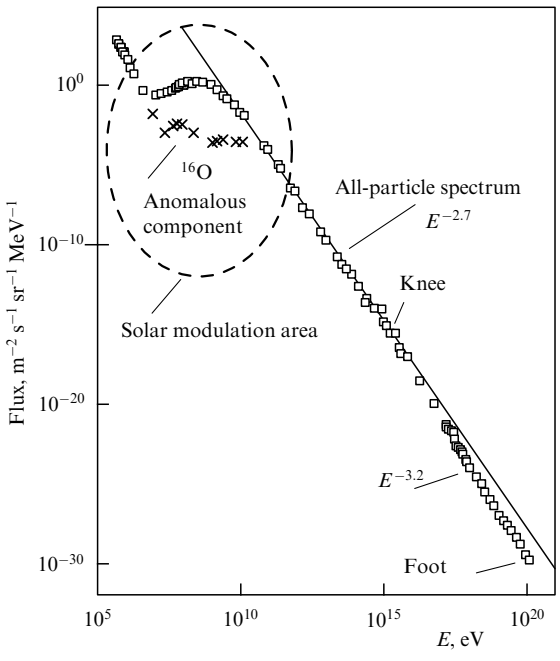

Figure 2. Differential energy spectrum of 'all' CR particles, not divided into individual components [29].

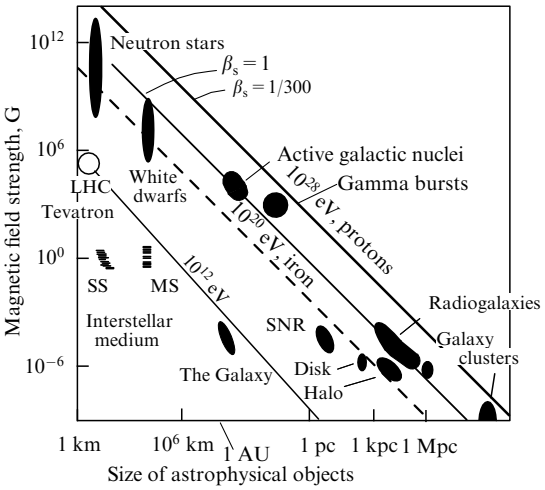

Figure 3. Hillas diagrams [44] demonstrating the capabilities of various astrophysical objects as particle accelerators. SNR is supernova remnants.

gauss) of objects capable of accelerating protons to 10^{20} and 10^{21} eV at an SW speed 300 times less than the speed of light. The dashed line shows the same for iron nuclei. Symbols SS and MS in Fig. 3 stand for sunspots (particle acceleration in the Sun) and magnetic stars (acceleration in other stars). The possibility of acceleration in the interplanetary medium is noted separately. For comparison, the figure also shows the characteristics of the two largest accelerators operating on Earth: the Tevatron and the Large Hadron Collider (LHC). The main conclusion following from the Hillas diagram is that there is apparently no viable candidate for the role of a particle accelerator to energies of 10^{20}–10^{21} eV in the Universe.

Let us also mention the so-called Hillas rule: the Larmor radius of a particle must not exceed the size of the acceleration region; otherwise, the accelerated particles would simply leave it. The same natural condition also determines $E_{\max}$ (up to 10^{17} eV) for GCRs accelerated in supernova remnants. Dark spots in Fig. 3 represent observable astrophysical objects, shown together with their size (in parsecs) and magnetic fields (in gauss). We note that the maximum energy of particles (protons) attained in modern ground-based accelerators does not generally exceed 10^{12} eV. Only on June 3, 2015 at the LHC at CERN was it for the first time possible to accelerate protons to 1.3×10^{13} eV; the projected maximum energy is 1.4×10^{13} eV.

In the original Hillas diagram [44], possible losses due to synchrotron radiation are not taken into account (although this applies mainly to electrons and positrons). This effect was taken into account in [45], where a Hillas plot was supplemented by contraints due to radiative losses and the most recent data of astrophysical observations. Unlike the authors of previous studies, the authors of [45] emphasized that active galaxies cover a large area on the diagram, and only the most powerful of them (radio galaxies, quasars, blazars, and BL Lac-type objects) are capable of accelerating protons to ultrahigh energies. However, acceleration of heavier nuclei is possible in lower-power Seyfert galaxies, which are much more numerous. More specific sources of ultrahigh-energy accelerated particles are discussed in Section 7.

2.3 Anisotropy

As regards data on CR anisotropy, its degree depends on the considered energy range. Most of the CRs observed in the vicinity of Earth's orbit are distinguished by a high degree of isotropy, but the intensity at energies $\leqslant 10^{10}$ eV is affected by solar modulation. In the UHECR energy range, CRs can be accelerated in rather exotic objects such as neutron stars, quasars, and relativistic jets, which are generated by active galactic nuclei (AGNs). It is clear that CRs are then distributed in a highly anisotropic manner. Heavy nuclei must strongly deviate from their original direction after leaving the source and cannot therefore be used as a tool for exploring the distant Universe. But, on more modest spatial scales, heavy nuclei are very important for verification of acceleration models [29].

The small number of events, the relatively poor angular resolution, and the deflection of charged particles by cosmic magnetic fields make it currently impossible to identify UHECR sources object by object, as is customary in classical astronomy. Instead, the strategy is to use statistical methods and look for manifestations of specific source population models in the anisotropic distribution of CR arrivals for an overall sample of events. Searches for global and small-scale anisotropy can be distinguished here (see [46] for details).

Global anisotropy can be expected when the observed CR flux is due to a limited number of relatively closely spaced sources. This is possible in two cases: (1) a significant increase in the density of sources close to the observer; (2) particles from distant sources not reaching Earth for some reason. The first case corresponds to sources located in our Galaxy (truly *galactic* CRs; see Section 6). The second case relates to astrophysical sources of protons with energies close to the Greisen–Zatsepin–Kuzmin (GZK) limit; the dominant contribution to the CR flux at such energies must be determined by sources located inside the so-called GZK sphere with a radius of about 100 Mpc.

The anisotropy of solar cosmic rays is determined by specific features of the source itself (a coronal mass ejection (CME) or flare; see Section 5) and depends primarily on the energy of SEPs, their charge, and the curvature of the interplanetary magnetic field (IMF), especially at relativistic energies.

2.4 Observation methods

The means and methods for studying CRs [47] in the vicinity of Earth must be described, at least schematically. As can be seen from Fig. 4, truly primary CR particles can only be detected by SCs orbiting Earth and other SCs outside Earth's atmosphere and magnetosphere. Because CR particles differ in energies by a factor of $\sim 10^{15}$, studying them requires a variety of methods and detecting devices (Fig. 4a). Secondary particles (products of nuclear interactions of primary particles with the atmosphere) can be observed at various altitudes above sea level, on Earth's surface, and on mountains, and a strongly penetrating component (muons) can be observed in underground detectors. For example, extensive air showers (EASs) — abundant cascades of secondary particles (Fig. 4b) — are detected by ground-based facilities with a large area, sometimes reaching several hundred square kilometers; some of these facilities are located at high altitudes. Among domestic installations of this kind, we mention the Yakutsk and Baksan complexes for studying EASs. Well known are international projects such as the Pierre Auger Observatory (PAO) and the Telescope Array (TA).

In Earth's atmosphere, measurements are carried out using small balloons and large high-altitude balloons. Underground telescopes are located either deep below the surface or at great depths in lakes (for example, in Lake Baikal) and

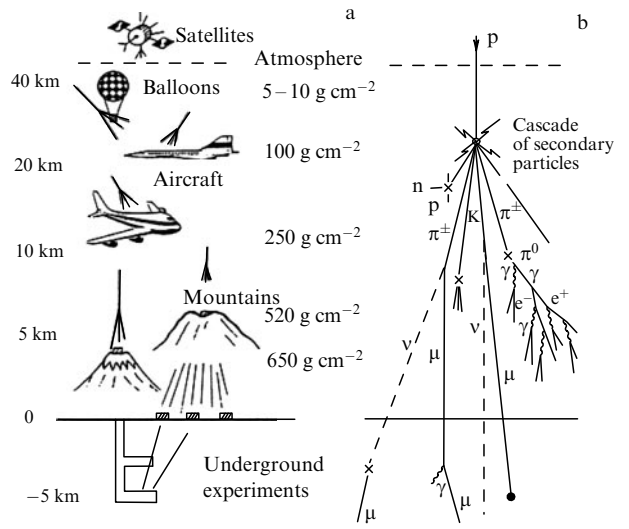

Figure 4. (a) Methods of CR observations [47] at different altitudes, on mountains, and underground. (b) Diagram of a nuclear cascade (EAS) in the atmosphere.

oceans, where only high-energy secondary particles, such as muons, penetrate (Fig. 4a).

Since the middle of the twentieth century (for more than 70 years), CRs have been continuously registered on Earth's surface by a worldwide network of stations studying CR variations with mainly standard neutron monitors (NMs) and standard and nonstandard muon telescopes (MTs). Ground-based observations of CR variations have allowed discovering SWs in interplanetary plasma (see, e.g., [10, 25, 27] and the references therein). The effect of SWs manifests itself in the form of a decrease in the GCR flux (the so-called Forbush effect, discovered in 1937). Valuable information about GCRs and SEPs is provided by observations at large nonstandard facilities such as the Baksan complex for studying EASs.

In recent years, huge installations such as IceCube in Antarctica have been used to address some astrophysical problems (for example, to search for astrophysical neutrinos and study the GZK effect). We note that facilities such as the Baksan complex and IceCube turned out to be sensitive not only to galactic but also to solar CRs. For example, the unique Baksan Underground Scintillation Telescope (BUST) registered a number of muon bursts whose nature remains unclear [10, 27] but which were associated with the arrival of solar CRs on Earth. In turn, at least one of the cases of the arrival of relativistic protons on Earth from the Sun, a GLE (ground level enhancement) event on December 13, 2006 [10], was simultaneously recorded not only by the ground-based network of CR stations but also by the Antarctic ground-based IceCube installation and the PAMELA (Payload for Antimatter Matter Exploration and Light-nuclei Astrophysics) orbital spectrometer detector.

3. Acceleration in Earth's magnetosphere

Near-Earth space (NES) was a subject of increasing interest among researchers long before the advent of the 'space age' (1957). Since the time CRs were discovered, high-altitude probe balloons have been widely used, and high-altitude rockets, etc., began to be used later on. Interest has increased many times when the NES studies started involving artificial satellites, space stations, interplanetary probes, etc. With the discovery of Earth's radiation belts (ERBs), it turned out that the NES could serve as an effective laboratory for testing models of charged particle acceleration. As is known, the NES simultaneously contains ionizing radiation components associated with the action of different sources and acceleration and transfer mechanisms.

3.1 Acceleration laboratory

Somewhat anticipating a discussion further on in this review, we note that several acceleration mechanisms are implemented in the NES at once: the betatron effect, acceleration by an electric field during magnetic reconnection, Fermi-type acceleration on a bow shock, etc. In addition, the magnetosphere, which is a very complex system in and of itself, contains neutral-layer electric fields, convective electric fields generated by fluctuating electric and magnetic fields, parallel electric fields in auroral zones, and various local wave–particle processes (see., e.g., [48, 49]). Moreover, it turns out that the magnetospheres of other planets show clear evidence of particle acceleration in auroral regions, magnetic tails, and equatorial regions due to electric fields, wave–particle interactions, and magnetic pumping (see, e.g., [50]).

The bow shock wave of Earth is the most studied example of a collisionless SW in the Solar System (see, in particular, [51]). This example is also widely used to model or predict SW behavior in other astrophysical conditions. Observations with SCs in conjunction with theoretical and numerical simulations have led to a detailed understanding of the structure of the bow SW, the spatial organization of the components that make up the SW interaction system, as well as fundamental processes associated with SWs (such as heating and particle acceleration). A review of observations of ions accelerated on and in front of Earth's SW is given in [51]. The models and theories used to explain SWs are discussed there. The global morphology of quasiperpendicular and quasiparallel shock and foreshock regions is described. Acceleration processes for beams oriented along the field and diffuse ion distribution types are discussed in connection with the foreshock morphology and shock structure. Possible mechanisms for the involvement of solar wind ions in acceleration processes are also described. It is noted that, despite several decades of research, some problems concerning ion acceleration on a bow SW have not been solved yet (see book [52]).

Despite the long period of research in this area, there are a number of gaps in the NES that have to be explored further. Radiation belts are not an exception in this regard (see, e.g., [53]). This highly dynamic area of the NES is an important natural laboratory for studying the physics of particle acceleration. Despite the proximity of radiation belts to Earth, many questions remain about the mechanisms whereby particles are rapidly accelerated there to relativistic energies. The importance of understanding radiation belts continues to grow as society becomes more dependent on SCs for navigation, weather forecasts, and more. The historical and observational foundations of our current understanding of particle acceleration in radiation belts are discussed in [53]. Fast local acceleration of relativistic ERB electrons by magnetospheric *very low-frequency* (VLF) chorus-type radiation is considered in [54].

Geophysicists from the Polar Geophysical Institute, jointly with Czech colleagues, have recently studied low-frequency choral emissions in Earth's magnetosphere.

Choral emissions play an important role in the dynamics of ERBs that can harm SCs. Scientists have noted the following pattern: waves propagating towards the geomagnetic equator have a higher frequency and lower amplitude than those moving away from it. This regularity was explained based on the theory of generation of choral radiation constructed previously in Russia [55]. Geophysicists have thus confirmed their hypotheses about the formation of such signals in space plasma. The global statistical response of the external ERB during geomagnetic storms was studied in [56]. The fast acceleration of ERB electrons during a specific geomagnetic storm on July 16, 2017 was simulated in [57].

Empirical estimates of the lifetimes of ERB electrons were recently compared with theoretical estimates [58]. In this case, quasilinear diffusion rates due to pitch-angle scattering by various mechanisms in electron ERBs were calculated. The theoretically calculated lifetimes turned out to be in good qualitative agreement with empirical estimates. The general structure of the observed electron lifetime profiles was a function of their energy and the altitude of the L-shell (where L is the geocentric distance in units of Earth's radius R_E to the point of intersection of the dipole geomagnetic field line with the equatorial plane). The specified profile structure was also seen to be largely caused by plasmaspheric hiss (radio noise caused by natural atmospheric processes, primarily lightning discharges) and Coulomb scattering.

Characteristically, the results of the comparison indicate the existence of a local minimum of the lifetime in the inner zone at lower energy ($\sim$ 50 keV), which is usually assumed to result from enhanced scattering due to terrestrial transmitters operating at very low frequencies. The decrease in the lifetime at higher L and higher energies (> 1 MeV) is then attributed to an increase in the scattering of electromagnetic cyclotron waves of ions. In addition, the authors of [58] found a significant quantitative discrepancy at $L < 3.5$, where the theoretical lifetimes are usually ~ 10 times longer than the observed ones, which indicates an additional loss process that is overlooked in modern models. Possible factors that may contribute to this disagreement were discussed in [58].

The source of most ERB particles is known to be located near the outer ERB boundary, in the range of geostationary SC orbits, at distances of 6 to 7 Earth radii. On the whole, however, the picture of the spatial distribution of trapped particles and the particle acceleration pattern in the magnetosphere and the variations of trapped radiation turned out to be so complex that in the context of this review we have to restrict ourselves to only the most typical facts and generally accepted models. Of particular interest is the fast local acceleration of electrons to relativistic energies [54].

The main problem — particle acceleration during a magnetospheric substorm — was solved in a series of studies by a group of researchers [59–62] who first developed a three-dimensional numerical model of the behavior of the geomagnetic tail in the magnetohydrodynamic (MHD) approximation in the presence of purely ohmic resistance. The model shows how the tail becomes unstable and forms a thin layer with subsequent reconnection of magnetic field lines at a distance of about 20 R_E downstream from the solar wind plasma flow along the tail. It is this thin current sheet that produces anomalous resistance due to the instabilities generated by the current and hence provides the conditions for subsequent reconnection. A plasmoid is then formed and ejected along the tail (see, e.g., [63] for the magnetic substorm of April 18, 1974). A substorm current wedge forms simultaneously inside the tail, and a key moment, called *dipolarization*, comes when the reconnecting field lines of elongated shape in the growth phase rapidly move toward Earth, resembling a spring, and return to a configuration closer to the dipole one. A similar process is also observed in solar flares, which is then called loop collapse (details and references to the literature on this subject can be found, e.g., in book [64] and paper [65]).

The problem of identifying an acceleration mechanism that transforms the small thermal energy of the solar plasma (of the order of 1–10 keV) into particle energy, which in ERBs reaches approximately 1000 MeV for protons and 10 MeV for electrons, was shaped by the early 1960s. The mechanism was found just a few years after the discovery of the radiation belts themselves.

The theoretical model that explains almost the entire spatial–energy structure of ERBs was created by the mid-1960s. It is based on the diffusion mechanism of particle transfer across the magnetic field (i.e., in the radial direction) under the action of fluctuations in the NES electric and magnetic fields. The productivity of this approach is testified by the fact that the radial diffusion mechanism is currently considered the main one for explaining the experimentally observed temporal and spatial–energy distribution of trapped particles inside Earth's magnetic trap.

3.2 Theory of radial diffusion

The radial transport of particles is caused by fluctuations in electric and magnetic fields in the magnetosphere, and the fluctuations themselves are caused by changes in the solar wind pressure. The induced electric field leads to particle drift in crossed magnetic and electric fields. This results in the diffusion transfer of particles across the magnetic field lines (Fig. 5). After moving inside the trap, the particles increase their energy via the betatron mechanism but preserve their magnetic moment (the first adiabatic invariant) $\mu = p_\perp^2/B = \text{const}$, where $p_\perp^2$ is the particle transverse momentum squared and $B = 0.312/R_E^3$ is the local magnetic field induction (expressed in gauss) in the plane of the geomagnetic equator. This shows that, when drifting toward Earth, a particle increases its energy in inverse proportion to the cube of the distance of the particle drift shell from Earth: $E \sim R_E^{-3}$. Particles from the magnetotail, which is a kind of reservoir of solar wind and ionosphere plasma (see below for more on this source), therefore fall into a magnetic trap and are accelerated in the process of being transported into the interior.

The idea of particle diffusion inside a magnetic trap in the presence of magnetic field disturbances such as sudden pulses was first proposed by Parker in 1960 [66]. Subsequently, the idea of diffusion transfer has been developed in many studies (see, e.g., [67–74]). This process is precisely diffusion, which means that particles preferentially move inside ERBs. Such a transfer is described by the Fokker–Planck equation, whose solution gives a picture of the spatial–energy structure of the trapped radiation in the form of the particle distribution function.

A fundamental role in the diffusion equation is played by the diffusion coefficient, which determines the speed of particles moving across magnetic field lines. In approaching Earth, particles feel the increasing impact of various loss mechanisms. From the standpoint of the radial diffusion concept, this leads to the appearance of intensity maxima of certain ERB particles at their fixed energies (Fig. 6).

Numerous studies have shown that the model of 'magnetic diffusion' (i.e., the transport of particles under the

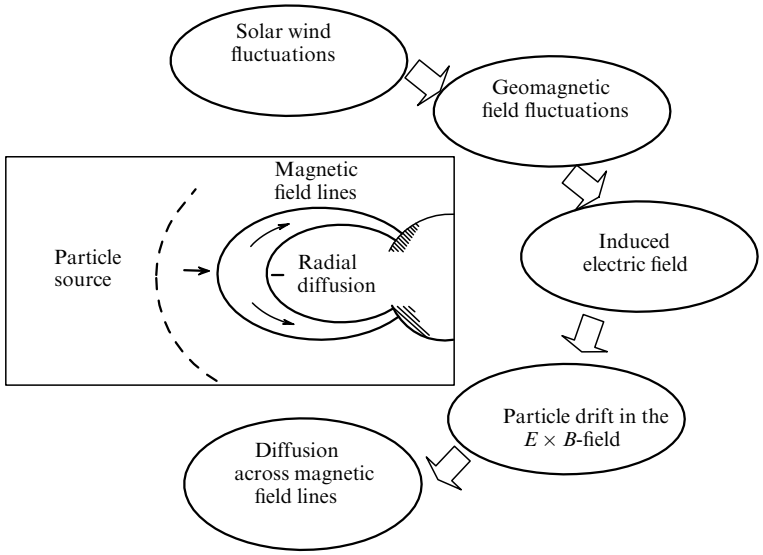

Figure 5. Physical process in the inner magnetosphere leading to radial diffusion of particles in the magnetosphere [29].

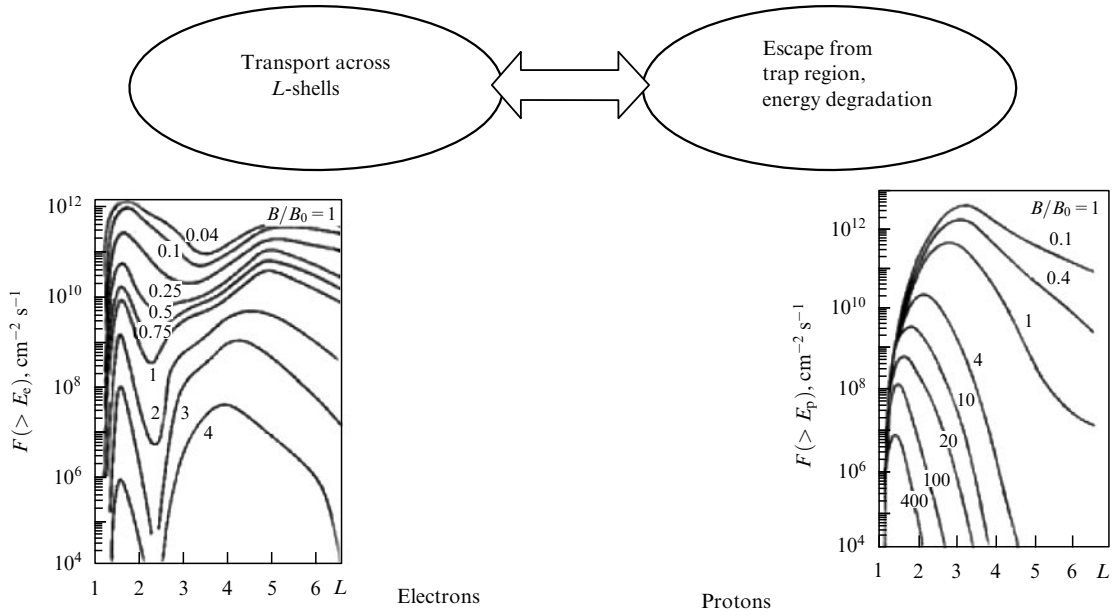

Figure 6. Formation of the spatial–energetic structure of radiation belts of electrons and protons resulting from the balance between their transport velocity across magnetic drift shells (L) and particle losses [29]; F is the particle current. Numbers on the curves show energies E_e and E_p for electrons and protons in arbitrary units; B is the dipole magnetic field induction at a given point, and B_0 is the dipole magnetic field induction at the apex of a field line.

action of magnetic field fluctuations) with the diffusion coefficient proposed in [67, 69–72] does indeed describe most of the temporal and spatial–energy structure of ERBs. In other words, magnetic diffusion plays a dominant role in the radial transport of particles. As a result, on the inner magnetic shells (at distances of less than $2R_E$ in the equatorial plane), a very energetic ion belt is formed, consisting of particles that are present in the solar wind and the ionosphere. The energy of captured protons in this region can reach 1 GeV, which is comparable to the GCR energy.

3.3 Ionospheric injector

Special mention should be made of the ionospheric source of trapped radiation. This source (an 'ionospheric fountain' of particles such as nuclei of oxygen) was first discovered in the early 1970s during observations on an American polar-orbit satellite [75–79]. After these observations, it became clear that the sources of ERB particles are not only solar but also ionospheric plasma. Subsequently, it was shown (see, e.g., [80]) that ions originating in the atmosphere can be divided into two groups. In the first, oxygen O^+ is most abundant, which is associated with substorm activity, whose intensity changes with the solar cycle: in particular, it increases as solar radiation increases in the extreme ultraviolet (UV) range (wavelength $\lambda = 25$–135 nm). This range is often referred to as 'extreme UV radiation' of the Sun. The second group consists mainly of H^+ and $^2He^+$ ions, which are especially numerous in geomagnetically quiet periods and do not show a significant dependence on the level of extreme UV radiation from the Sun. As regards acceleration processes associated with ionospheric ions, electrostatic acceleration in double layers and turbulence act as effective acceleration mechanisms there. The charge exchange theory [81] then leads to the conclusion that the particle composition becomes heavier as

particle energy increases, and the charge distribution at $L < 5$ should be independent of the ion source.

The decay of albedo neutrons produced by the interaction of GCRs with the atmosphere is an additional mechanism that ensures the filling of the inner zone of trapped radiation by high-energy protons. Heavier particles arise here as products of nuclear reactions in the interaction of primary GCR protons and ERB inner zone protons with Earth's atmosphere.

The most self-consistent theory of particle acceleration in alternating magnetic fields was developed in [73, 74]. There, the scattering of particles by hydromagnetic turbulence was proposed as a scattering mechanism, and the problem of particle acceleration was posed in terms of the equations of quasilinear kinetics. This allowed determining both the spectrum of accelerated particles and the spectrum of turbulent fluctuations that cause particle scattering. In particular, the mechanism of so-called Alfven magnetic pumping [82], whereby an exponential increase in the average particle momentum due to betatron acceleration and nonadiabatic scattering by hydromagnetic turbulence is possible in a turbulent plasma, was discussed in [74]. This possibility is realized with a slow periodic change in the magnetic field in a turbulent plasma.

In the framework of the acceleration problem under consideration, heavy charged particles with sufficiently large energy losses that can cause failures and disturbances both in biostructures and in SC electronics are of particular interest. The region of localization of such particles is the inner zone of ERBs.

3.4 Contribution of ions coming from planetary atmospheres

There is another HZE source in the NES: anomalous CRs captured in the magnetosphere (see, in particular, [28, 29, 83–85] and references therein). Due to the use of data obtained by Cosmos series SCs, a model of the spatial distribution of the belt of captured ACRs (actually, a new radiation belt near Earth) was constructed [86–88]. These observations showed that interstellar matter is in fact present inside Earth's magnetosphere, in the form of captured ACRs.

As regards the acceleration of charged particles inside the magnetosphere and in the regions of its interaction with the solar wind, many researchers note the similarity of accelerating processes in solar flares and in the magnetosphere. As noted, for example, by an international group of researchers [89], the acceleration mechanisms operating in the auroral zones of Earth are still not fully understood, although several theories and models (sometimes competing with each other) have received experimental confirmation in recent decades. The authors of [89], in particular, emphasize the role of parallel electric fields generated by quasistationary or Alfven processes.

3.5 Ring current and particle acceleration

Of particular interest for particle acceleration in the NES is the ring current (RC) [90] in the magnetosphere, which is the cause of geomagnetic storms (see, e.g., [91, 92]). Experiments on the satellites Explorer 45, Molniya 1, Molniya 2, and other SCs back in the 1970s indeed confirmed that, in the energy range from several ten keV to 200–300 keV, protons are the most important component of the RC, responsible for its energy characteristics. It turns out that variations in the density of particles of just this component of near-Earth radiation correspond to the Dessler–Parker–Skopke formula (see, e.g., [93–95]) that relates changes in the geomagnetic field and the stored energy of RC particles.

In contrast to particles of the radiation belts, RC particles are more susceptible to the action of the magnetospheric electric field (see [96–98] and references therein). Therefore, the detection of the longitudinal asymmetry of the RC at the initial phase of a magnetic storm was quite natural from the standpoint of the model of particle drift in crossed electric and magnetic fields (see Fig. 5).

The role of magnetospheric electric field variations in the dynamics of particles inside the trapping zone was considered in detail by Tverskoy in 1969 (see [71] and also [72, 99]), and the characteristic features of the RC dynamics during magnetic storms became an additional argument supporting this model.

3.6 Difficulties with acceleration in the magnetosphere

As an illustrative example of the 'difficulties' that arise in the study of particle acceleration in the magnetosphere, we present the results of observations aboard the AMPTE–CCE (Active Magnetospheric Particle Tracer Explorers–Charge Composition Explorer) SC. Based on the data in [100], in Fig. 7 we show the ion flux ratios near the ERB boundary (ring current) after a substorm to the corresponding fluxes before the onset of the substorm for H^+, He^{2+},

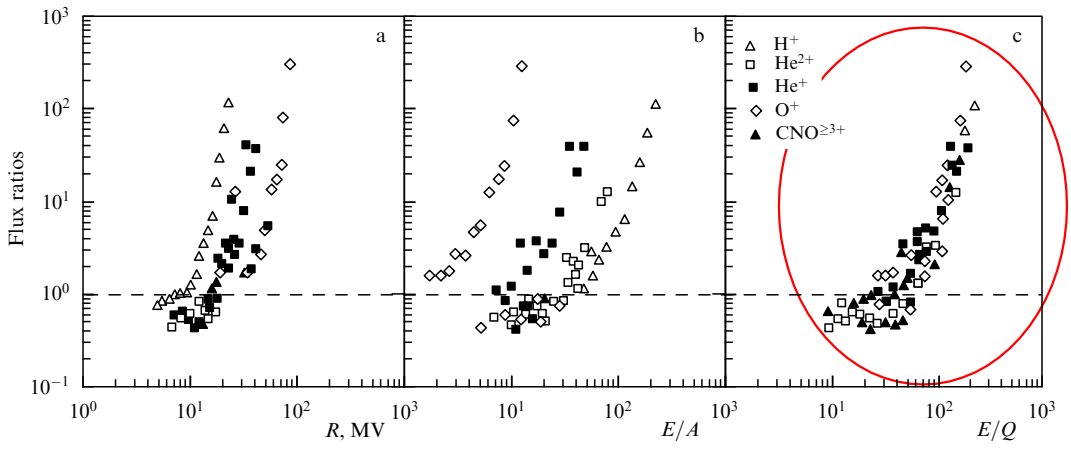

Figure 7. Data from observations aboard the AMPTE–CCE SC by the CHEM (Charge Energy Mass Spectrometer) detector [100]. Shown are ratios of ion fluxes after a substorm to those before for the ring current ions H^+, He^{2+}, He^+, O^+, and $CNO^{\geq 3+}$ as functions of (a) rigidity R, (b) the energy-to-mass ratio E/A, and (c) the energy-to-charge ratio E/Q. Oval shows the grouping of particles by the value of E/Q.

He^+, and O^+ ions and for CNO $^{\geqslant 3+}$. The ratios are presented as functions of rigidity R, the energy-to-mass ratio E/A, and the energy-to-charge ratio E/Q.

It turns out, in particular, that the spectra of ions included in the composition of RC particles tend to line up in accordance with the E/Q ratio, and not according to the rigidity R of the particles or according to the E/A ratio. Such a trend may indicate the presence of processes that depend on the E/Q ratio, for example, acceleration by an electric field.

4. Anomalous component of cosmic rays

The anomalous component of CRs in the heliosphere (see Fig. 2) was discovered in the early 1970s from SC measurements. The ACRs include light hydrogen ions H and heavier ions He, C, N, O, Ne, and Ar and possibly S, Si, and Fe with energies up to $\sim$ 50 MeV per nucleon; they are observed in the interplanetary space and in Earth's magnetosphere. The chemical composition of this CR component differs from the solar and galactic abundances of elements; for example, some excess of carbon relative to oxygen is sometimes observed.

4.1 Discovery and origin of anomalous cosmic rays

In Fig. 8, we show typical energy spectra of oxygen nuclei measured by various detectors aboard the ACE (Advanced Composition Explorer) SC (see review [101] and paper [102]). Other ions tend to have similar spectra. The curves in Fig. 8 correspond to solar wind particle fluxes, including the extrapolation of fluxes for a 'stable' state of the interplanetary medium (the postulated 'quiet' background of superthermal solar particles); to the high-speed flow of solar wind; to the particle flux due to solar wind corotation processes; and to a flow of energetic storm particles (ESPs), solar CR flows, and an anomalous component of GCRs and the GCRs themselves. The energy ranges of various instruments aboard the ACE are given in [103]. At the bottom of Fig. 8, we show the measurements to be made by the different ACE instruments.

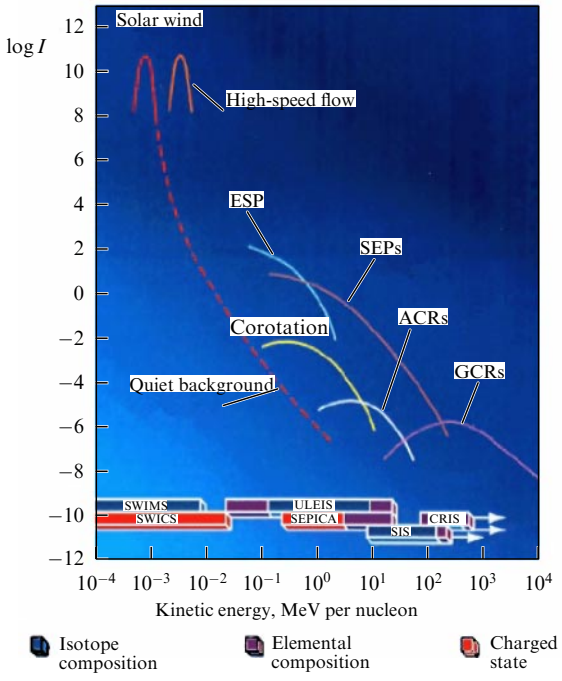

Figure 8. (Color online.) Typical energy spectra of oxygen ions representing different particle populations in the heliosphere. Lower part shows what kind of measurements are assigned to ACE instruments: SWIMS (Solar Wind Ion Mass Spectrometer), SWICS (Solar Wind Ion Composition Spectrometer), SEPICA (Solar Energetic Particle Ionic Charge Analyzer), ULEIS (Ultra-Low-Energy Isotope Spectrometer), CRIS (Cosmic Ray Isotope Spectrometer), and SIS (Solar Isotope Spectrometer). (Image adapted from [101].)

Due to the rotation of the Sun around the galactic center, the interstellar environment at the edge of the heliosphere changes. This leads to changes to the structure and expansion of the heliosphere, as well as to the intensity of CRs and neutral gas fluxes. On the other hand, in the local interstellar medium (LISM), the inflow of the neutral component of the interstellar gas into the heliosphere occurs almost unhindered and, in the case of sufficiently large fluxes, can change the chemistry of planetary atmospheres.

The interplanetary space probes Voyager 1 and Voyager 2 (hereafter, V1 and V2), launched in 1977, are known to have played a special role in the study of ACRs. Both probes long ago crossed the Solar System boundary: V1 crossed the boundary of the heliosphere in December 2004, and V2, in August 2007. This happened at the respective distances of 94 and 84 AU from the Sun. Since then, both vehicles appear to be moving in an LISM dust cloud in which the Solar System is immersed (the so-called Local Bubble).

4.2 Intial concept of acceleration

According to [104], ACRs began to appear in observations about 40 years ago. Within a few years, a concept explaining their origin was developed. The ACRs were assumed to begin their life in the form of interstellar neutral atoms drifting into the heliosphere. Then, these atoms become singly ionized [105] via either charge exchange with solar wind ions or photoionization. The formed ions are then 'picked up' by the expanding solar wind and are accelerated to observable energies by the diffusive shock acceleration (DSA) mechanism (see Section 5.3) on the terminal shock wave of the solar wind (also called the boundary SW). In what follows, we refer to it as TW for brevity.

This first concept of ACR particle acceleration was widely accepted and stood the test of further observations until December 16, 2004, when V1 crossed the TW, but found no source of ACRs. In August 2007, V2 crossed the TW elsewhere, but did not find the location of the ACR source either. It became clear that the location of the ACR source had nothing to do with the TW that both SCs had crossed. Alternative models have been proposed that assume acceleration elsewhere in the TW and/or other accelerating processes in the heliosheath.

4.3 Modern models

According to [104], ACR fluxes in the range of medium and higher energies measured aboard V2 as of 2013 exceeded the fluxes measured aboard V1, but the V2 spectra were more strongly modulated. This fact supports theoretical models in which the ACR source is placed along the TW flank or tail [106, 107], because V2 is farther away from the heliosphere 'nose' than V1 (Fig. 9). According to [104], the fact that the ACR energy spectra measured by V2 appear to be more modulated than those measured by V1 may be due to the difference in the rigidity dependence between the diffusion coefficients in the case of V2 (a southern source) and in the case of V1 (a northern source). Although the observations are qualitatively consistent with the ACR source being located

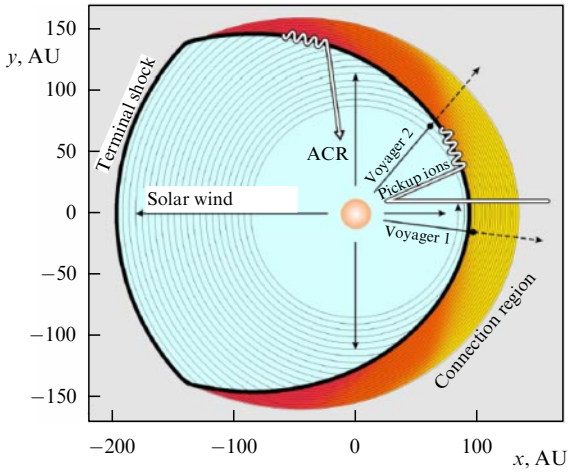

Figure 9. (Color online.) Asymmetry of the heliomagnetosphere and the generation of ACRs [106]. Connection region is regions of reconnection, pickup ions refers to ions picked up by the solar wind.

along the TW flank or tail [106, 107], other models are now being considered, including acceleration in 'hot spots' of turbulent TWs [107, 108], acceleration at the heliopause due to magnetic reconnection [109, 110], and acceleration by the magnetic pumping mechanism, which mainly occurs near the heliopause [111]. Obviously, new observations are needed to clarify the nature and location of ACR sources.

4.4 Accounting for the geometry of the heliosphere

The difference between the distances at which the V1 and V2 SCs crossed the heliosphere boundary indicates an asymmetry in its structure (see Fig. 9). The asymmetry is due to the motion of the Sun in the interstellar space. Indeed, the Sun (together with the entire Solar System) moves in the interstellar gas relative to the nearest stars at a speed of ~ 20 km s^{-1}. Neutral interstellar atoms (interstellar wind) then penetrate into the Solar System and ultimately serve as a source of ACRs (see, e.g., [83] and references therein). According to modern concepts, ACRs are generated by the processes of recharging the penetrating atoms with solar wind particles and acceleration on a TW at the heliosphere boundary. In addition, it was found that ACR ions penetrating into Earth's magnetosphere produce a belt of trapped particles, whose formation mechanism is different from the traditional one.

The theory of ACR acceleration proposed in an early paper [112] states that ionized (in the past, neutral) particles can indeed be accelerated from an energy of ~ 4 keV per nucleon to more than 10 MeV per nucleon just at the heliopause (at the TW) if they are 'picked up' by the solar wind. Another (alternative or complementary) approach amounts to the assumption that the ACR source is the ionospheric plasma of magnetic planets enriched in O^+ ions. In addition, we recall (see Section 3) that interstellar matter is actually present inside Earth's magnetosphere (in the form of captured ACRs). The ERB consisting of ACR particles [29] is then located at a distance slightly longer than $2R_E$ in the equatorial plane. GCR particles with energies $E > 70$ MeV (protons) have shown that the TW had already passed and both V1 and V2 plunged into the LISM several years ago [29].

We note that, at present, there are also two long-lived space probes in space: Pioneer 10 and Pioneer 11, launched back in the 1970s, but with other goals and moving in the 'opposite' direction than that of V1 and V2.

The last contact with Pioneer 10 occurred on January 22–23, 2003. At that time, the SC was at a distance of 82.19 AU from the Sun and moving away from it with a relative speed of 12.224 km s^{-1}. The further fate of Pioneer 10 is unknown, but it is assumed that it continues to fly and will eventually leave the Solar System, heading toward Aldebaran.

The last signal from Pioneer 11 was received on September 30, 1995. After that, the orientation of its antenna to Earth was lost and the SC cannot maneuver to recover it. Whether Pioneer 11 continues to transmit signals is unknown, and no further tracking is planned. It is assumed that Pioneer 11 is heading toward the Aquila constellation and will pass near one of its constituent stars in about 4 million years.

4.5 Acceleration in the interplanetary medium

In relation to the analysis of possible sources of ACRs, it seems appropriate to discuss the possibility of accelerating charged particles in the interplanetary medium itself. This is especially interesting in application to particles passing structures such as corotating interaction regions (CIRs) of two solar wind streams of different speeds. Such structures are regularly present in interplanetary space.

The data shown in Fig. 10 refer to the SEP event on March 22, 2000. On that day, a corotating region enriched with solar particles ^{4}He, C, O, and Fe was observed in the interplanetary space by the ACE SC at a distance of about 1.5 mln km from Earth [113, 114]. In considering the total-energy spectra, we can clearly see the trend toward enrichment of the accelerated particle stream with heavy ions (Fig. 10b). It is interesting to check the acceleration model proposed in [115] using these data just when CIRs are present in the interplanetary space.

We note that, in the interplanetary medium, similarly to the case of solar flares, magnetic reconnections of oppositely directed magnetic fields occur. A combination of two mechanisms can be at work here: DSA (see Section 8) and direct acceleration of particles by electric fields arising in the process of magnetic reconnection (see, e.g., [116, 117]).

5. Solar cosmic rays

Among the nearest sources of cosmic radiation, solar cosmic rays (SEPs) are apparently studied the best (albeit far from being fully understood). Indeed, the Sun emits charged particles in a wide energy range, from thermal particles of the solar wind (the so-called coronal evaporation) to relativistic electrons, protons, and heavier nuclei (ions), which are accelerated in flares and/or at SW fronts produced by CMEs. Neutrinos are also generated in the interior of the Sun. These facts allow testing various astrophysical theories, ranging from models of nuclear processes in the interior of the Sun to models of the solar dynamo and acceleration.

5.1 Observational data

The general pattern of the distribution of solar wind, GCR, and SEP particles observed near Earth's orbit is shown in Fig. 11 (using relative flux units). We can immediately see from Fig. 11 that these particle populations (especially the GCRs and SEPs) are quite different in their characteristics. In addition, the SEP fluxes themselves vary widely. Of particular interest are events with relativistic particles (mainly protons, but also heavier nuclei), GLEs. This name, standing for

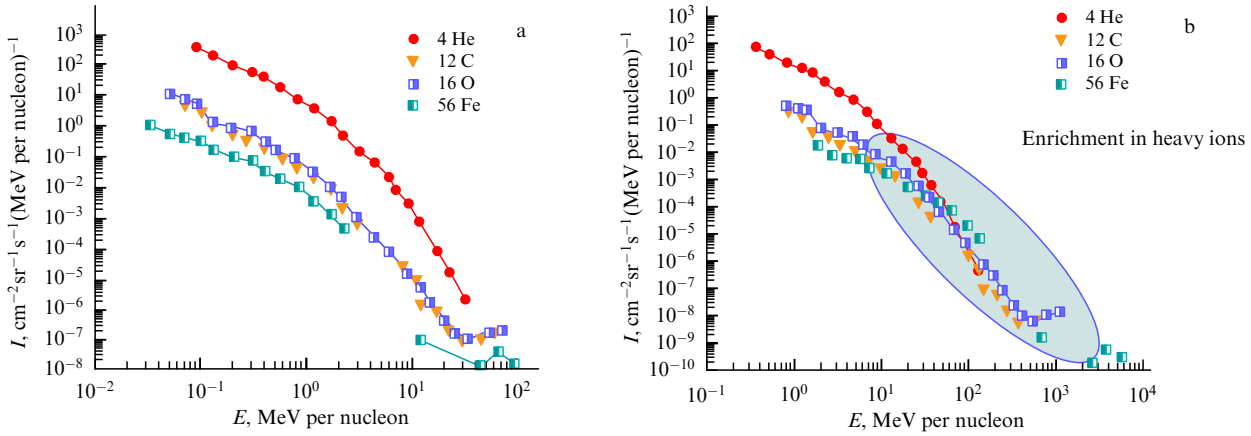

Figure 10. (Color online.) Spectrum of ^{4}He, C, O, and Fe ions obtained by ULEIS and SIS detectors aboard ACE in observations of the corotating region on March 22, 2000. (Image adapted based on data in [113, 114]; see also review [101].)

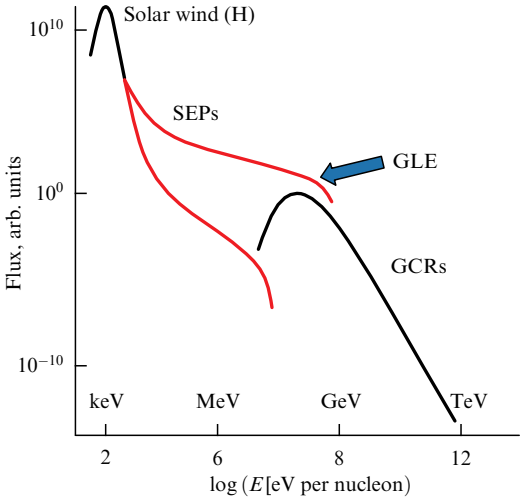

Figure 11. (Color online.) General pattern of the distribution of solar wind, GCR, and SEP particles [29] observed near Earth's orbit (expressed in arbitrary flux units).

ground level enhancements, has been in use since the early 1990s for ground-based increases in the SEP flux [10, 27], which, after 1942, were recorded by ionization chambers (ICs), and since the 1950s, mainly by NMs and MTs. There are currently two widely used GLE databases: the European Neutron Monitor Data Base, http://www.nmdb.eu, and an international database, https://gle.oulu.fi.

The debate about the sources of SEP particles appearing in the IMF after an explosive release of energy on the Sun has been ongoing for several decades (see, e.g., [10, 25, 27, 118–121]). As is known, the main candidates for the role of SEP sources are solar flares and CMEs. The debate has not given a clear advantage to any of the possibilities, but brings more and more new facts that complicate understanding the true picture. For example, the focus in [120] is on recently discovered new manifestations of sudden energy releases on the Sun. These include long-term (so-called pion) high-energy gamma radiation (> 90 MeV) and new data on solar neutrons and terahertz radio emission. The description of particle acceleration on the Sun turns out to be even more complicated [120] than previously thought.

Until recently, there was a tendency to study SEPs separately from CRs of other origins (see, e.g., monograph [17] and [10, 25, 26, 122]). The authors of [17], while analyzing the mechanisms of acceleration in space conditions, focus mainly on GCRs and largely ignore SEPs and the effects of GCR modulation, not to mention the observational aspects. This approach is quite justified in view of the SEP features noted above. On the other hand, many researchers (see, e.g., [121] and references therein) use their own terminology for energetic particles of solar origin and focus on the SEPs. We emphasize that the term SEP includes all solar CRs (see, e.g., [42]), from HZE ions of nonrelativistic energies to relativistic electrons and relativistic protons with energies of ≈ 20–30 GeV (and possibly $\geqslant 100$ GeV) (see [26]).

Regarding acceleration mechanisms, the problem as a whole is of a *general* physical nature. We nevertheless find it more convenient to separately discuss the adduced arguments pertaining to the peculiarities of SEP acceleration.

We first note that the study of SEPs turned out to be very fruitful for the development of the theory of acceleration in general. For example, some SEP events in the relativistic SEP (proton) energy range have spectral-temporal features that allow associating them with a possible *first-order* Fermi acceleration (see Section 8) between converging SWs in interplanetary space. In particular, according to [123], such events took place on July 17, 1959, on November 12, 1960, and on August 4, 1972. It is possible that similar events were also observed on October 19, 1989 and on July 14, 2000 (the BDE, Bastille Day Event) (see, e.g., [10, 123] for details).

5.2 Features of acceleration

We note the most characteristic features of SEP acceleration. In our opinion, they include the following points.

(1) Poorly known and dynamically (rapidly) changing initial and 'boundary' conditions in the solar atmosphere. The dynamical model of SEP spectrum formation proposed many years ago [124, 125] (see also [126]) may partly resolve this difficulty. At any rate, the model in [124, 125], given the properties of the source, allows estimating the relative contribution of the betatron effect compared with the contribution of acceleration by the electric field in the magnetic reconnection region.

(2) The (generally) variable shape of the observed SEP spectrum, including the presence of features such as the exponential *turnover* of the power-law spectrum, or in other terms similar in meaning, a break-off, a cutoff, a bend, or a knee. These features are discussed in more detail in [10, 126–

128]. In view of the importance of this issue, we discuss it in Section 5, in conjunction with the results in [127, 128].

(3) Of special interest are the observed 'bumps' in SEP spectra (see, e.g., [129]) in the nonrelativistic energy range (the SEPs proper). The existing models of acceleration on SWs cannot yet explain this effect. Some prospects may be associated with a combination of direct acceleration by an electric field and betatron acceleration [124, 125] (also see [126]).

(4) For energy reasons, the integrated SEP spectrum must necessarily have a 'cutoff' [27]. In this regard, we note that the frequently used particular approximation in the form of a double power-law function [130] does not have sufficient physical justification in application to SEPs [122, 131]. Nevertheless, in many cases, it should be acknowledged that it yields a good description of empirical (experimental) results in various areas of space research, including SEP spectra in limited energy intervals.

(5) The so-called magnetic reconnection (reconnection of oppositely directed magnetic fields; see, e.g., [22, 64, 65, 132, 133]) plays a special role in SEP generation, when conditions arise in the solar atmosphere for direct acceleration of particles by electric fields. As noted, it cannot be ruled out that magnetic reconnection occurs not only in the solar atmosphere but also in the interplanetary medium. A combination of two mechanisms then operates: the DSA (see Section 5.4) and direct acceleration of particles by electric fields arising from magnetic reconnection [116, 117]. Some of the noted features of SEP acceleration are illustrated below with specific observational data.

5.3 Injection problem

It has been recognized recently that the elemental composition of SEPs and the charge state of heavy charged particles are key to understanding the processes of particle acceleration on the Sun. The most problematic case is HZE acceleration, but even then the study of SEPs has brought some clarity when taking the peculiarities of their propagation into account (see, e.g., [134, § 14] and also [135]). As is known, the path characterizing the scattering of particles on IMF inhomogeneities depends on the magnetic rigidity of the latter. This leads to a difference between the velocities of protons and those of heavier nuclei by about a factor of two in the region of nonrelativistic energies. Hence, observations near Earth's orbit must show the spectrum of solar particles enriched with heavy nuclei over time. For GCRs, on the other hand, the problem of nuclear injection (first noted by Fermi [13]) remains unresolved.

As was subsequently noted in [18], the injection energy scales as $E_i \propto Z^2$. This means that the injection energy for heavy nuclei is much higher than for protons. Hence, it should also be expected that the HZE contribution to the total flux of accelerated particles would be negligibly small. But, as shown by numerous observations (see Fig. 1), the situation is just the opposite: in the GCR composition, the content of heavy nuclei in relation to their composition in sources is much higher than for protons (see, e.g., [15, 17, 18, 134]).

To solve this problem, the authors of [136] back in 1959 took into account that, if the background plasma temperature is not too high, the heavy ions must be singly or doubly ionized, and hence the real acceleration starts from the effective charge $Z^* = 1$ or 2, which makes the HZE injection energy close to the proton injection energy. With an increase in energy, the effective charge also increases, but the increase in energy in any accelerating process exceeds the ionization losses. Moreover, according to the authors of [136], if the acceleration starts with a speed $v < v_e$, where v_e is the speed of background plasma electrons, then the injection energy level is immaterial, and practically all particles with this speed take part in the accelerating process. The modern approach to the injection problem is discussed in Section 9.3.

For SEPs, the problem is further complicated by the fact that the observed composition and charge state of accelerated nuclei (HZE ions) change significantly from one SEP event to another and appear to be substantially dependent on the altitude at which the acceleration source is located in the solar atmosphere (Fig. 12). In a number of papers [137, 138] (see also [139]), attention has long been drawn to the fact that, as HZE particles are accelerated, their charge state changes with time: heavy ions are 'stripped off' by thermal protons from the environment. Previously, this effect was erroneously almost completely ignored, although in reality it is a decisive ingredient.

To overcome the difficulties associated with changes in the SEP (including HZE) composition, some researchers (see, e.g., [140]) propose that the height in the solar corona at which particle acceleration occurs in a particular SEP event be taken into account. The geometry of SWs in the solar corona must also then be taken into account by including the possibility of generating quasiperpendicular and quasiparallel SWs.

In Fig. 12, we show a scheme where the main processes associated with a solar corona flare are combined: magnetic reconnection, particle acceleration, CME generation, the formation of quasiperpendicular and quasiparallel SWs, etc. The composition and charge state of accelerated HZE particles are then determined by the conditions (height, composition, and temperature) at the source. For example, a quasiperpendicular wave accelerates particles with the coronal composition, while a quasiparallel wave accelerates solar wind particles. This scheme was used, in particular, by the authors of [140] to explain the HZE composition from solar flares, at least for so-called gradual SEP events.

In the standard CSHKP (Carmichael–Sturrock–Hirayama–Kopp–Pneuman) flare model (see [142] for details), magnetic reconnection in the CME wake gives rise to a two-ribbon flare.

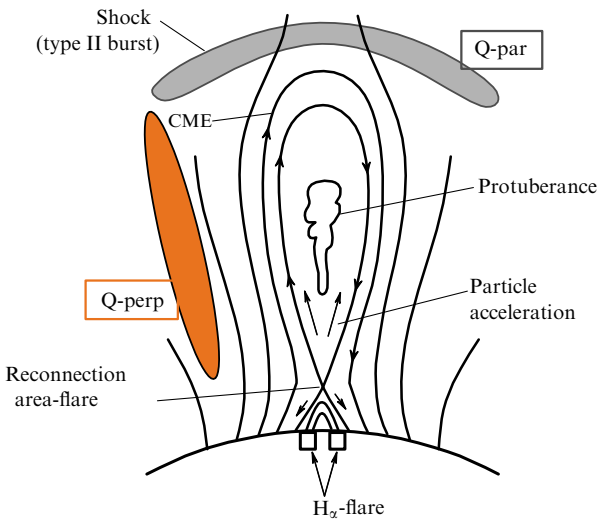

Figure 12. Possible scheme of the formation of quasiparallel (Q-par) and quasiperpendicular (Q-perp) SWs in the solar atmosphere in the course of a solar flare [141].

If the flare particles are not captured by the CME, they can become a 'seed' for acceleration by a quasiperpendicular wave (see Fig. 12).

We also note cases of the detection of SEP particles coming from so-called narrow CMEs. For example, the authors of [143] report two SEP events that were observed by the ERNE (Energetic and Relativistic Nuclei and Electrons) instrument aboard SOHO (Solar and Heliospheric Observatory). Both events were pulsed with an intensity above 10^{-3} protons/(cm^2 s sr MeV) in the energy range of several ten MeV and were associated with CMEs with an angular width less than 60° and a linear velocity greater than 800 km s^{-1}. One of the events was not related to a solar flare. This means that the first injected protons were entirely produced by the associated CME. In the second case, a pulsed solar flare of class M1.1 was observed. The calculated time of the first injection for $\sim$ 36 MeV protons propagating over a distance of 1.2 AU was close to the time of the CME start. These observations are inconsistent with the view, expressed in some studies, that narrow fast CMEs are not associated with SEP events.

5.4 Acceleration on shock waves

On the other hand, if we turn to the well-known DSA mechanism (see Section 8 for details), the maximum energy of particles accelerated by an interplanetary SW is determined by the SW deceleration rate, its 'age,' and IMF attenuation with distance from the Sun. According to some estimates (see, e.g., [144]), the DSA mechanism only provides the maximum energy of accelerated particles of the order of 1 GeV in Earth's orbit if the wave is 'young.' This value decreases to $\sim$ 100 MeV (for protons) at a distance of 2 AU.

The DSA mechanism was first used to study the SEP problem in [145], where a linear version of first-order Fermi acceleration was considered. Linearity means that the flow of accelerated particles does not affect the SW itself. Under some simplifying assumptions, the authors of [145] obtained an equation for the SEP differential spectrum in the form of a power-law function times an exponential:

$$\frac{\mathrm{d}F}{\mathrm{d}E} = D_0 E^{-\gamma} \exp\left(-\frac{E}{E_0}\right). \quad (1)$$

The authors of (1) consider this equation suitable for describing the spectrum of both solar electrons with energies starting from 100 keV and GLE protons with energies up to 10 GeV. We note, however, that when applied to SEP generation (i.e., acceleration in the solar corona and interplanetary medium), this mechanism has serious limitations [146]. In particular, its implementation requires the so-called injection energy (i.e., pre-acceleration).

Interesting information was obtained in the ACE SC orbit during the GLE66 event, which was observed by the global network of CR stations on October 29, 2003 (Fig. 13), as well as by proton detectors aboard SC GOES-11 (Geostationary Operational Environmental Satellite 11) [147–149]. The data from the SIS, ULEIS, and EPAM (Electron, Proton, and Alpha Monitor) instruments aboard the ACE SC and from the Energetic Particles Spectrometer detector aboard GOES-11 were used (see [148, 149] for details). The ion flux for each element was multiplied by a scaling factor to separate the spectra. The authors compared their measurements of the SEP nuclear composition aboard ACE with measurements of proton fluxes near Earth (GOES-11). They interpreted the data on the basis of the acceleration model [145].

In accordance with the model in [145], an exponential cutoff should be clearly seen in the energy spectrum of protons and heavier ions, which we do see in Fig. 13. Such a result, however, contradicts the data in Fig. 10. On the other hand, this does not mean that the processes of acceleration in the interplanetary medium must be identical to those in a solar flare. The values of E_0 in Fig. 13b obtained from the data presented in Fig. 13a are shown as functions of Q/M. For elements with $Z \geqslant 2$, the dependence $(Q/M)^{1.75}$ is obtained, which is similar to the theoretically expected one, but somewhat weaker [150].

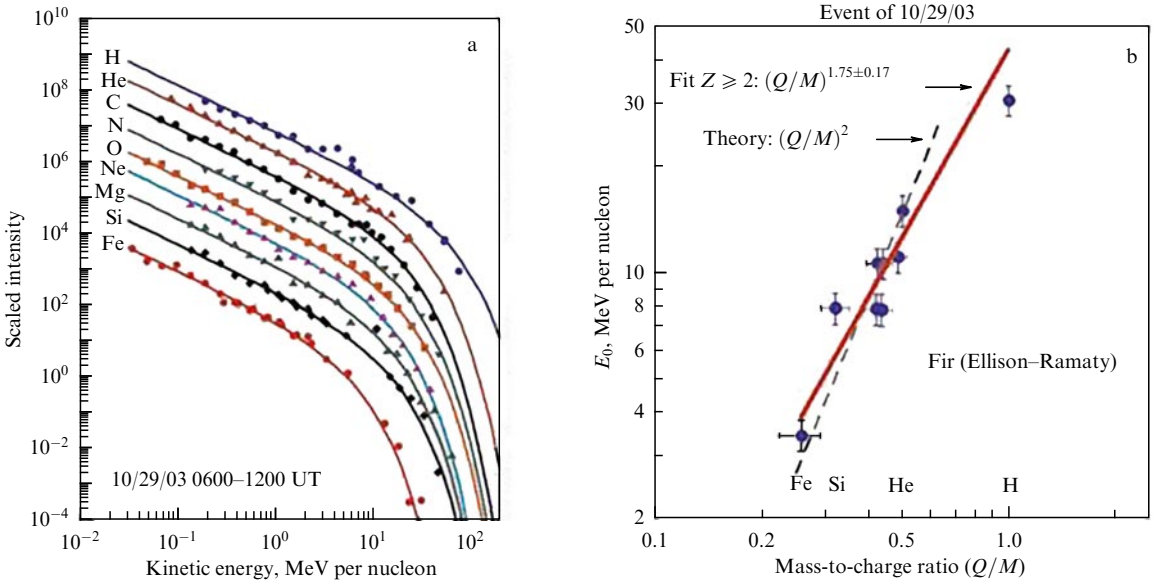

Figure 13. (Color online.) (a) Spectra constructed based on the ACE data for 6-hour intervals after the SW passage observed on October 29, 2003 [147–149] presented in a power-law approximation [145] with a fixed exponent equal to −1.3. (b) Values of E_0 from formula (1) obtained from the data in Fig. a, depending on the value of Q/M.

Recently, in a series of papers [151–155], data on ground-based measurements were used to study the question of the sources of accelerated particles in so-called weak GLEs, also called sub-GLEs, in the 24th solar activity cycle. The aim of the study was to test the hypothesis that acceleration occurs on SWs. Four models of this kind have been considered ([115, 155–157]). The first of the models in [115] describes acceleration in interplanetary space, as shown in Fig. 10. When compared with the data for sub-GLEs, it turns out that none of the models is capable of unambiguously explaining the observed features of the SEP spectra. New data on particle fluxes in different SEP energy ranges are needed, especially measurements of weak fluxes of relativistic protons (see, e.g., [155] and references therein).

To give an example, in Fig. 14, we show the results of an analysis of the maximum integrated intensities $I_{\max}(>E)$ for the sub-GLE on January 6, 2014 [153]. This SEP event was observed by both the ground-based network of NMs and satellite detectors. Figure 14 shows the integral spectra of protons from GOES-13 measurements (up to 100 MeV) and estimates of the absolute intensity of relativistic particles from the NM data [153]. It can be seen that approximation (1) proposed in [145] has to be significantly refined with data from the 'intermediate' energy range of 200–300 MeV, notably using new instrumental capabilities for SEP observations at the Antarctic Concordia station [158, 159].

The last example, which illustrates difficulties with the SW acceleration model applied to SEPs in the DSA framework, is shown in Fig. 15 [129]. Among the features of the energy spectrum of the October 28, 2003 event (GLE65), the above-mentioned bump is clearly visible in the energy range of 4–80 MeV. The horizontal lines in Fig. 15 show the widths of the respective differential energy channels; vertical is/are measurement uncertainties of SEP fluxes. Curve *1* is the approximation of the spectrum by the function $J(E) = 350E^{-1.4}\exp(-E/450)$ [particles/(cm^2 s sr MeV)]. Curves *2–4* are the results of different variants of calculations according to model [157] (see [129] for the details).

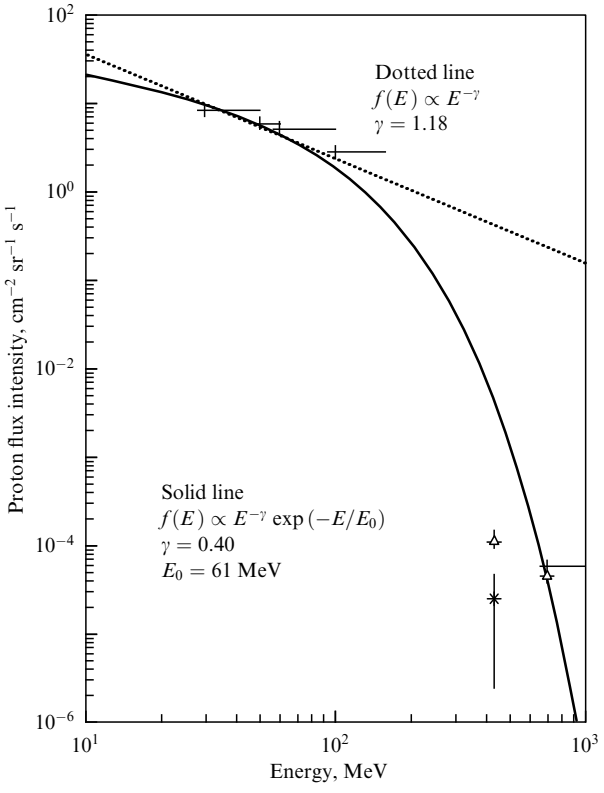

Figure 14. Integrated spectrum of maximal intensities obtained based on data from several detectors aboard the GOES-13 SC, shown together with spectral estimates based on NM data [153] for the sub-GLE on January 6, 2014. Solid curve shows the spectrum approximation in accordance with the model in [145].

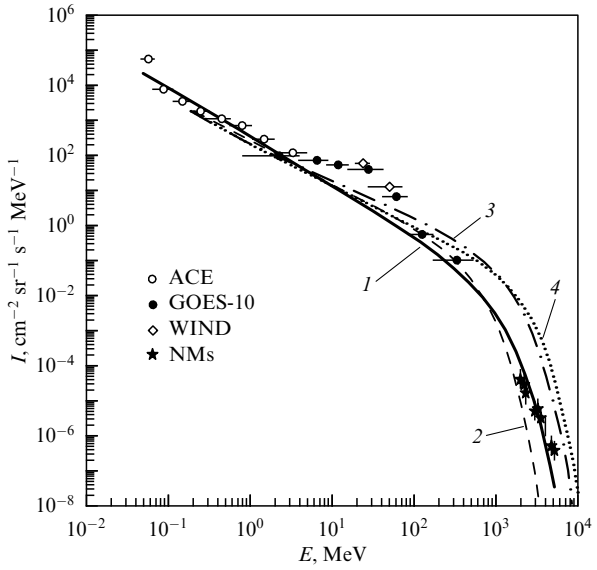

Figure 15. Energy spectrum of SEPs at 14:00 UT, October 28, 2003 (isotropic stage of GLE) in the maximally wide energy range [129] based on measurements by ACE (circles), GOES-10 (black dots), WIND (diamonds), and NM networks (stars).

Despite the above critical remarks, we note in general that, in our opinion, the researchers from Yakutia have implemented the most detailed and consistent approach to the problem of SEP sources within the DSA framework. They considered two versions of the theory, linear [156] and nonlinear [157] (see also [129]). Recent semiempirical data on the altitude profile of the plasma density and on the level and spectrum of Alfven turbulence in the solar corona (based on radio observations of solar flares) have been taken into account. Theoretical calculations were then brought to the final formula describing the shape of the resulting SEP spectrum:

$$N(E) = N_0 E^{-\gamma}\exp\left[-\left(\frac{E}{E_{\max}}\right)^{\alpha}\right]. \qquad (2)$$

Here, N_0 is a normalization factor and $E_{\max}$ is the characteristic energy of the spectrum. Expression (2) contains a power-law part with the exponent $\gamma \approx 2$ (which is comparable to the estimate in [145]) and an exponential tail with the parameter $\alpha \approx 2.3 - \beta$, where β is the exponent in the spectrum of coronal Alfven waves.

According to [156, 157], $E_{\max}$ can vary in a wide range, 1–300 MeV, depending on the SW speed. With the example of several SEP events, the authors showed that the above formula describes the SEP spectrum well in the nonrelativistic region, but is apparently not suitable for describing the relativistic part of the spectrum. As noted previously in [146], when describing the spectrum in the case of GLE42 (September 29, 1989) for energies above 1 GeV, even at the

late, isotropic stage of the event, i.e., essentially, only for the spectrum of the slow component, the Yakutian model gives rather uncertain results, which strongly depend on the exponent of the Alfven turbulence spectrum $\beta = 0.5$–1.5. The fast anisotropic component, which was clearly identified in the GLE42 event (see, e.g., [160]), was not considered at all in [156, 157].

One of the latest studies in this field [129], devoted to analyzing the large GLE65 (October 28, 2003), cannot give a satisfactory answer to all questions about the formation of the SEP spectrum either. The authors of [129] again analyze only the slow SEP component detected at 14:00 UT (see Fig. 15), already in the period of event isotropy. With reasonable accuracy, the resulting SEP spectrum can be approximated by the function $D(E) = 350 \times E^{-1.4} \exp(-E/450)$ [cm^{-2} s^{-1} sr^{-1} MeV^{-1}]. Importantly, a bump is clearly seen in the observed spectrum in the energy range of 4–80 MeV. The nature of such features, which are often observed during acceleration on SW fronts under various astrophysical conditions, was repeatedly discussed previously [129, 154, 156, 157, 161], but there is still no complete clarity on this issue.

Among the attractive results in [129, 156, 157], the one most important to us is a self-consistent acceleration scenario applicable in the range from the generation of SWs in the corona to the formation of the SEP spectrum. The acceleration process ends at a distance of several solar radii R_S. For example, in the powerful GLE65 event mentioned above, acceleration ended at a height up to $4R_S$ [129], i.e., below the zone of the solar wind outflow from the surface of the Sun. This does not contradict the estimates of the SW generation and CME formation height in [156, 157]. On the other hand, we note that the strong anisotropy at the GLE start indicates the emission of relativistic particles from a point-like source, such as the flare itself, rather than from a longitudinally distributed source such as an SW.

How do these theoretical results correlate with observations? As an example, we consider data on one of the SEP events (GLE71 on May 17, 2012) observed in the 24th solar activity cycle by the STEREO (Solar Terrestrial Relations Observatory) SC [162]. The authors of [162] assume that the onset of type II solar radio emission in the VHF band corresponds to the moment of SW and CME generation at a distance of $1.38R_S$ from the center of the Sun. The height of the CME at the time of emission of GLE particles in this event, according to direct STEREO data, was $2.32R_S$. This height agrees with the values for the GLE events of the preceding cycle 23 obtained by the backward extrapolation method.

5.5 Elemental composition and charge state

Does the SEP spectrum contain a tail enriched in heavy nuclei? This question is one of the key ones in the SEP acceleration (origin) problem. It has been the subject of numerous papers, both physical and statistical in nature (for details, see, e.g., books [27, 121]). We have already seen above (Fig. 12) what kind of difficulties arise in the study of this question. Below are the most characteristic data on the elemental composition and charge state of SEPs.

Over more than 25 years of almost continuous observations with the CRT (University Chicago's Cosmic Ray Telescope) instrument, a unique database of high-energy solar HZE particles has been obtained (see, e.g., [140, 163]). In large-scale SEP events, the IMP-8 (Interplanetary Monitoring Platform 8)/CRT telescope even detected solar Fe ions in the GCR background with an energy up to ~ 800 MeV/nucleon. This database, in particular, has allowed comparing in [163] the proton spectra deduced from NM data (with energies above 500 MeV) during the GLE on September 29, 1989 [164] with the data of simultaneous measurements of solar Fe ions in the energy range of ~ 50–1000 MeV/nucleon in the CRNC (Chicago's Cosmic Ray Nuclear Composition experiment) aboard IMP-8 (Fig. 16).

The spectra of protons and Fe ions obtained from observations with the CRT instrument are shown in Fig. 16a as functions of the total energy per particle. Solid curves are

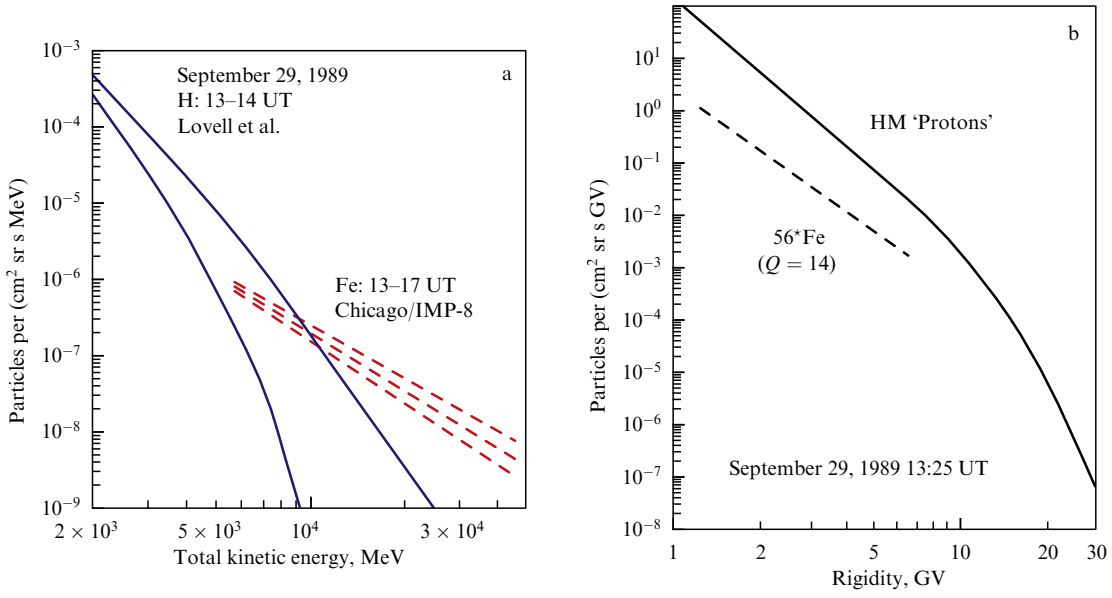

Figure 16. (Color online.) Spectra of relativistic solar protons and Fe ions with an energy greater than 100 MeV/nucleon, constructed from (a) energies and (b) rigidities based on data from measurements during the GLE on September 29, 1989 [163]. Solid blue curves in Fig. a show the estimates in [164] (J L Lovell, M L Duldig, J E Humble, 1998).

estimates for the upper and lower bounds of the proton flux in the time interval of 13:00–14:00 UT, obtained, according to [164], from data from ground-based NMs. Dashed curves correspond to Fe ions with the uncertainty of the chosen spectral exponent taken into account.

The measurements in [163] allowed detecting the hardest spectrum of solar Fe ions ever observed. If we consider the spectra as a function of rigidity, then the flux of Fe nuclei is apparently insufficient to complicate the interpretation of the results of NM observations, even when taking the partial charge state of iron ions (~ 14.0) into account. But, at very high total energies, the spectrum of iron nuclei is much harder than that of protons; both protons and Fe ions then make apparently comparable contributions to the so-called all-particle spectrum. We note that, during GLE events, the contribution of HZE particles to the NM count rate in the background of GCR particles remains an unsolved problem and still attracts the attention of researchers (see, e.g., [165]).

Since the launch of the ACE SC (1997), detailed studies of the energy spectra of SEP particles have become possible in a wide energy range. As noted, two instruments for measuring heavy-ion SEP fluxes were installed aboard the ACE: ULEIS (E from ~ 0.01 to ~ 5 MeV/nucleon) and SIS (E from ~ 5 to ~ 200 MeV/nucleon). However, after analyzing the SIS data for 56 events, it was found in [127] that the spectra of ions from helium to iron are strictly power-law ones and have the same spectral exponents on average, which contradicts the conclusions in [147], where the data of all energies were analyzed for a specific event on October 29, 2003 (see Fig. 13). Moreover, according to [128], so-called inflections or kinks occur in the SEP spectra (Fig. 17), where the spectral exponent changes significantly, with $\gamma_1 < \gamma_2$. The energy of the middle of the inflection for both the averaged spectra and individual events depends on the type of particles and increases as the ratio A/Q decreases, where A is the atomic number and Q is the charge of an SEP ion, $E_0 = 14.5(Q/A)$ [MeV/nucleon] on average. Both the difference between and ratios of the spectral exponents γ_1/γ_2 are independent of the particle type on average. As regards the kinks (knees) in general, we have already expressed our opinion: the cause of kinks may turn out to be purely methodological (see point 2 in Section 5.2).

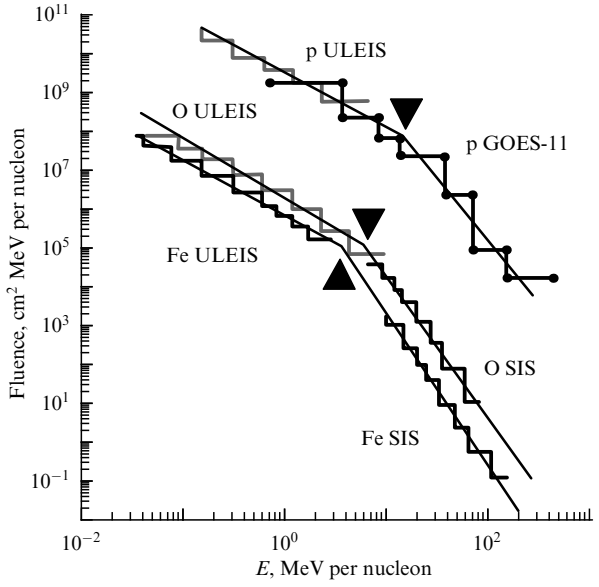

Figure 17. Logarithmically averaged fluences for 28 SEP events and their approximating spectra for protons, oxygen, and iron. Filled triangles show the inflection points [127, 128].

We now briefly consider the most recent results on this subject. As is known, at present it is difficult to separate the dependence of the acceleration parameters on the rigidity R from the rigidity transport effects of SEPs. It can be very difficult to separate these two groups of dependences. A previous proposal (see, e.g., [121] and references therein) was to divide all SEP events into 'gradual' and 'pulsed'. They do indeed differ in a number of characteristics (see, e.g., [27] for details), which recently allowed the author of [166] to propose a new tool for the separation of solar HZE particles and for studying the possible effects of SEP enrichment with heavy ions. Their mass-to-charge ratio A/Q, or, more precisely, the exponent δ of their ratio $A/Q \sim R^{\delta}$, can serve as such a tool. Magnetic reconnection in solar flare-jets (i.e., in pulsed events) gives positive values of δ in the range from 2 to 7, and acceleration on a SW (gradual events) yields mostly negative values, from -2 to $+1$, in small and moderate SEP events, in which transport effects are minimal.

The acceleration effects are dominant in those cases where the SEP events are weak or ions propagate without scattering. By contrast, the transport effects can dominate in large events during the time evolution of SEP fluxes at intensities close to the 'flux saturation' limit (see, e.g., [167]). According to [166], the rigidity dependence of the spectrum (i.e., the exponent δ) in the weakest and moderate SEP events is almost completely determined by the acceleration, and transport effects make almost no contribution. In pulsed SEP events, the exponent δ ranges from 2 to 7, and possibly from 2 to 5 for larger events, with a corresponding CME being fast enough to allow re-acceleration on the SW.

In [168], the same author investigated the relation between SEP energy spectra and the elemental composition. The study was carried out under the assumption that physical processes, both during acceleration on SWs and in the course of scattering during transfer, can lead to a correlation of spectral exponents with an increase or decrease in the abundance of elements, depending on the mass-to-charge ratio A/Q. Correlations have been noted for those gradual SEP events in which SWs accelerate ions from the ambient coronal plasma. However, there are no such correlations in 'pulsed' events caused by magnetic reconnection, and the increase in abundance lies in the range from $(A/Q)^2$ to $(A/Q)^8$. Such correlations are absent even if the SWs additionally accelerate (reaccelerate) these residual 'pulsed' ions. In one of the events, the spectrum of oxygen nuclei changed from $\sim E^{-1}$ to $\sim E^{-5}$, while the corresponding abundances varied from $(A/Q)^{+1}$ to $(A/Q)^{-2}$ during the event. These facts can serve as a stimulus for a new analysis of the 'injection problem' [169].

6. Galactic cosmic rays

The Hillas rule allows estimating the maximum energy $E_{\max}$ for GCRs accelerated in supernova remnants. This value is about $\leqslant 10^{17}$ eV (until the start of the 'foot'). We can see from Fig. 2 that, if the modulation region (energies below 10^{10} eV) is excluded from consideration, then the GCRs occupy at least five to six orders of magnitude in energy. The maximum energy of particles (protons) obtained in most modern ground-based accelerators is typically less than 10^{12} eV. We recall that only on June 3, 2015, at the LHC at

CERN, were protons first accelerated to energies 1.3×10^{13} eV (with the design maximum energy of 1.4×10^{13} eV).

This is not intended to disprove the great value of the information that can be gleaned by studying interactions at ultrahigh energies, still inaccessible to accelerators, by indirect methods, for example, by EASs. We also emphasize that astrophysical research in the range of ultrahigh energies requires certain assumptions to be made about hadronic interactions (see Section 9). In Sections 6.1–6.3, we discuss the most important data on the CR spectrum and composition obtained over the past two to three decades.

6.1 Principal sources: spectrum and mass composition measurements

The upper bound of the energy range where direct methods are applicable is approximately 10^{15} eV. This bound is based on the natural requirement of achieving reasonable statistical accuracy within a reasonable time of the experiment.

Supernovae are traditionally considered to be the main sources of GCRs; we refer, in particular, to books [15, 17, 170]. In addition to these fundamental monographs, a number of detailed reviews on the physics of CR acceleration and propagation have been published over the past decade, especially covering the UHECR range [39, 46, 171–173] (see also dedicated site [174]).

More specifically, GCRs are particles that have been accelerated by SWs in supernova remnants. In [171], the energy densities of various components of our Galaxy are given for comparison: cosmic rays, the magnetic field, star light, gas motion, and the microwave background (with a temperature of 2.7 K). It turns out that all components have comparable energy densities, about 0.5 eV cm^{-3}. Of course, a factor such as the microwave background cannot be attributed only to our Galaxy, because it is present everywhere in the Universe. As the authors of [171] note, the presence of a 'feature' in the CR spectrum, i.e., the lack of smoothness in it, is evident (see, e.g., Fig. 2). In their opinion, this supports the assumption that most CRs come to Earth from discrete sources, the most likely of which are supernova remnants. The last word remains with observations, however, and in Sections 6.1–6.3 we present the most interesting experimental results obtained in recent years.

Especially significant progress in the study of the energy spectrum and mass composition of primary CRs was achieved in the ATIC (Advanced Thin Ionization Calorimeter) balloon experiment (see, e.g., [175] for a description of the detector). An experiment carried out at the Skobeltsyn Research Institute of Nuclear Physics (NIIYaF), Lomonosov Moscow State University (MSU), in collaboration with scientists from the USA, South Korea, and Germany, was designed to measure the composition and energy spectra in the energy range from 5×10^{10} to $\sim 10^{14}$ eV per particle with element-wise resolution by a charge from protons to Fe nuclei. The contribution of the NIIYaF staff consisted in the development and construction of a charge detector that allowed obtaining undistorted information about the charge of each particle under conditions of a large flux of backscattered secondary particles from the calorimeter.

The ATIC instrument made three stratospheric flights around the South Pole in the period from 2000 to 2008. The total flight duration was about 50 days. The main scientific results [176] were obtained from the data from the ATIC-2 flight (2000–2003). A conclusion was drawn about a difference between the mean slopes of the spectra of protons and helium: the helium spectrum turned out to be more gently sloped. It was also noted that the proton spectrum is not described by a single power law: starting with energies above 10^{12} eV, the spectrum is more gently sloped than with lower energies, and then becomes noticeably steeper in the energy range above 10^{13} eV. The energy spectra of C, O, Ne, Mg, Si, and Fe nuclei have been measured. The spectra of all particles were measured in the energy range from $\sim 2 \times 10^{11}$ to $\sim 1.5 \times 10^{14}$ eV. An excess in the GCR electron flux was also found in the energy range above 200 GeV [177, 178].

It is clear that heavy nuclei must strongly deviate from their original direction after leaving the source. Therefore, they cannot be used as a tool to study the distant Universe [29]. But, on more modest spatial scales, they are very important for verifying acceleration models.

6.2 Where is the bound of the spectrum of galactic cosmic rays located?

Figure 18 shows the spectra measured for the mean mass composition of primary CRs. According to several experiments (ATIC, Tunka, KASCADE (KArlsruhe Shower Core and Array DEtector), and JACEE (Japanese–American Collaborative Emulsion Experiment)), the measured mean mass composition of CRs (Fig. 18a) indicates a possible enrichment in heavy ions. This trend is supported by data from other experiments (Fig. 18b).

Data on the mass composition of CRs obtained in the ATIC experiment, in particular, indicate the complex structure of this composition, depending on the particle energy. In any

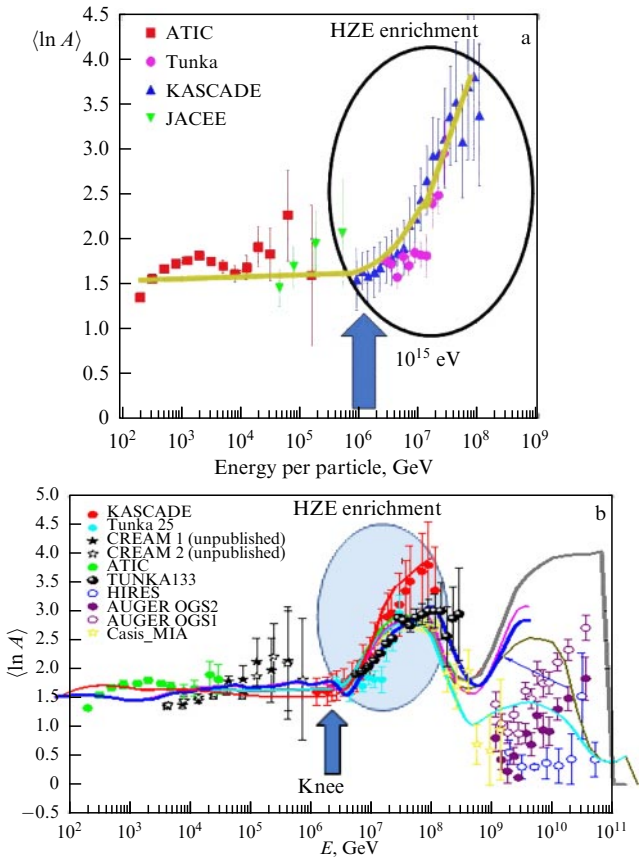

Figure 18. (Color online.) Assumed enrichment of the CR composition with heavy elements according to data from (a) four and (b) ten different experiments in the energy range beyond the knee [29]. Intensity I is expressed in arbitrary units.

case, in Fig. 18a and 18b, we can identify the energy ranges where the CR composition enrichment in heavy charged particles can be expected.

6.3 Heavier composition with increasing energy?

As is known, the mass composition of primary CRs can be determined from the results of measurements of $\langle \ln A \rangle$, which characterizes the depth of maximally developed EASs. For a given energy of a primary particle, this quantity depends logarithmically on the mass of the nucleus that generates the shower. The accuracy of its determination is about 30 g cm^{-2} [29]. According to data on the depth of the shower maximum in the energy range of 10^{15}–10^{16} eV, the mean logarithm of the mass number, $\langle \ln A \rangle$, is approximately 1.75 at such energies. With a further increase in energy, the composition rapidly becomes heavier. Such an effect at energies above 10^{16} eV is observed in practically all experiments (see Fig. 18), but the spread of the data is quite large.

On the other hand, it was shown in [179, 180] that the accuracy of determining $\langle \ln A \rangle$ can reach 16 g cm^{-2}. However, only showers caused by primary CRs with the energy of 10^{17}–$10^{17.5}$ eV were considered. Based on these data, the authors of [179, 180] concluded that there is a significant light component of primary CRs (probably of a proton nature or mixed up to 80%).

It is natural to ask the question: how does the chemical composition of CRs correlate with the composition of stars in the Universe, in particular, our closest star, the Sun? The answer is given in the Table, which shows the relative abundance of various elements in the composition of CRs, in the Sun, and in stars (see also Fig. 1 and its description in the text).

We can see from the Table that the CR composition approximately corresponds to the abundance of elements in the Universe, except in two cases: first, significantly more light nuclei (Li, Be, and B) are observed in CRs, and, second, in the range of heavier nuclei (similar to Fe in atomic mass), the CR composition apparently becomes heavier than the composition of the Sun and other stars.

7. Extragalactic cosmic rays

It seems obvious that CRs can no longer be called 'galactic' starting with a certain energy. This energy is generally accepted to be $E > 3 \times 10^{18}$ eV [29]. Apparently, this is where the transition to extragalactic ultrahigh-energy CRs begins. How high is the energy of the most energetic cosmic particles detectable in ground-based experiments? As of now, this value is 3×10^{20} eV.

Currently, there are only three experiments in the world that are capable of studying EASs caused by primary particles with energies $E > 10^{19}$ eV [46]. These experiments are very different and each has its own strengths and weaknesses. They are the Yakutsk complex EAS installation (Russia), the Telescope Array (TA) in Utah (USA), and the Pierre Auger cosmic ray Observatory (PAO) in Argentina. Similarly to completed past experiments, these installations yield results that are not entirely consistent with each other. To discuss these results and resolve inconsistencies, international working groups were organized in 2012, with representatives of all three ongoing experiments. The first results of the work of these groups were discussed at CERN in the spring of 2012. Our further presentation takes these results into account as much as possible.

We note that the PAO and TA experiments have so far detected only six events with $E > 10^{20}$ eV, and the arrival directions of two of them coincide within the angular resolution uncertainty [181].

Table. Chemical composition of cosmic rays compared to the composition of the Sun and stars. Oxygen content is assumed to be 1.0 [29].

Element	CR	Sun	Stars
H	685	1445	925
He	48	91	150
Li	0.3	$< 10^{-5}$	$< 10^{-5}$
Be-B	0.8	$< 10^{-5}$	$< 10^{-5}$
C	1.8	0.6	0.3
N	< 0.8	0.1	0.2
O	1.0	1.0	1.0
Mg	0.32	0.05	0.04
Si	0.12	0.06	0.04
Fe	0.14	0.05	0.06

7.1 Extragalactic particles in interstellar magnetic fields

Trajectories of charged particles of any energy bend in interstellar magnetic fields. Even for particles with energies in the ultrarelativistic range (10^{18} eV and higher), the deviation from a straight line is noticeable at galactic distances. In a magnetic field of ~ 3 μG, the Larmor radii for particles with energies $> 10^{20}$ eV are ~ 1000 pc. In Fig. 19, in addition to the 'all-particle' spectrum, we show the scale of gyroradii (Larmor radii) of protons in a 3-μG magnetic field. At ultrahigh energies $E > 10^{19}$ eV, the radii of proton trajectories must exceed the size of the Galaxy, and it can therefore be asserted with near certainty that particles of ultrahigh energies are produced outside the Galaxy.

In Fig. 19, we can clearly see the knee at energy $E \sim 3 \times 10^{15}$ eV, as well as the foot. Particle fluxes sharply decrease as the energy increases: at $E \sim 10^{19}$ eV, only one particle is observed incident on an area of 1 km^2 per year. The same figure also shows why the Hillas rule works against the existence of so-called Zevatrons — particle accelerators to energies of 1 ZeV $= 10^{21}$ eV [29]. The main conclusion

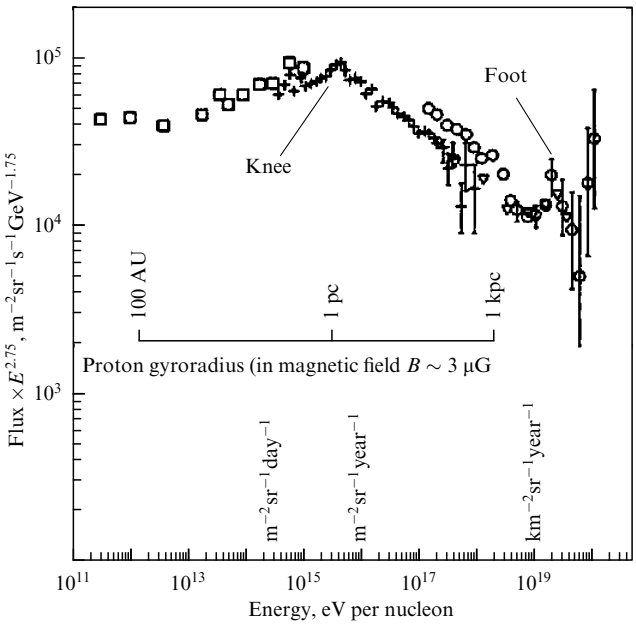

Figure 19. Differential energy spectrum of 'all particles' and scale of proton gyroradii in the interstellar field of ~ 3 μG [29].

following from the Hillas diagram is therefore that the Universe offers no clear candidate for the role of a particle accelerator to energies of 10^{20}–10^{21} eV.

As noted in [46], interest in the nature of ultrahigh-energy (more than 10^{19} eV) cosmic rays expressed by researchers working both in elementary particle physics and in astrophysics has not weakened for several decades. The problems arising in these fields relate both to the origin of particles of such high energies (not detected in nature under any other conditions) and to the search for new physics (see, e.g., [182]), which can manifest itself in the indicated energy range and can underlie the deviations of experimental results from theoretical expectations. As we see in what follows, these two groups of questions remain topical and even today largely determine the research strategy combining elementary particle physics and astrophysics.

7.2 Modern classification of spectrum features

Today, our ideas about particles with energies $\geqslant 10^{19}$ eV are as follows. On a double logarithmic scale, the 'all-particle' CR spectrum can be described as a superposition of several spectra: each successive leg differs from the preceding one by a change in the spectral slope exponent and, as has been established by now, by a characteristic change in their mass composition. In Fig. 20, we show the CR energy spectrum based on data from 14 modern experimental facilities. For obvious reasons, the accuracy of observations of ultrahigh-energy particles is not high, but, in our opinion, it still allows identifying several characteristic ranges in the CR spectrum.

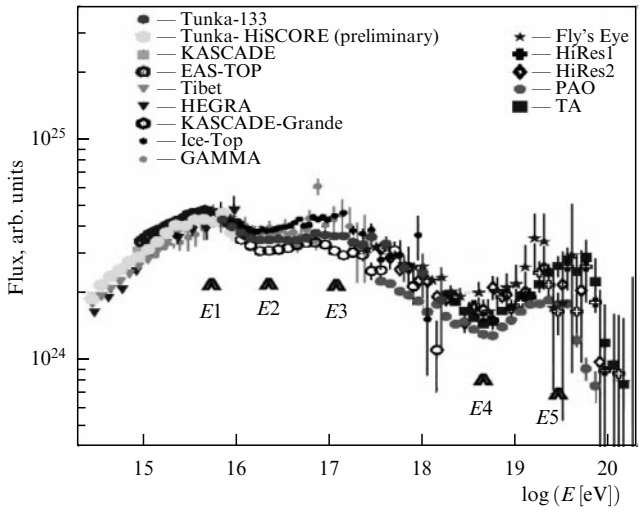

Figure 20. Differential energy spectrum of CRs in the range of high and ultrahigh energies based on data from 14 modern experimental facilities [29].

The astrophysical 'Khristiansen knee' [183] is denoted as $E1$ in Fig. 20. At present, thanks to measurements at ground-based EAS facilities, it has been established that the CR nuclear composition starts being enriched in heavy nuclei at energies $> E1$. In the energy range $> E1$, the spectrum is represented in accordance with data from the domestic ground-based facilities Tunka-133 and TAIGA-HiSCORE in comparison with data from other experiments.

More complex than previously thought, the nature of the CR spectrum in this energy range is one of the main results obtained in recent years at various modern facilities: Tunka-133, KASCADE-Grande, IceCube, and the Yakutsk facility. The CR spectrum exhibits two statistically justified features: at $E2 \approx 2 \times 10^{16}$ eV, the energy spectrum slope decreases, i.e., the spectrum becomes more rigid; at energy $E3 \approx 3 \times 10^{17}$ eV, the slope exponent again increases by about 0.3, i.e., the spectrum softens.

But at energies $E4 > 3 \times 10^{18}$ eV, the slope of the all-particle spectral curve again becomes more rigid: the so-called foot appears. It is noteworthy that, according to data from many ground-based facilities, it is in this region that the lighter CR fraction appears at energies $E > 10^{18}$ eV (Fig. 21). And at energies greater than $E5 \approx 5 \times 10^{19}$ eV, a sharp decrease in the CR flux is observed. Does this signify 'the end' of the CR energy spectrum? We note that the energy of an individual primary particle is currently estimated with a statistical error of $\approx$ (15–20)% and a systematic uncertainty of $\approx$ 25% [46].

In the area beyond the 'knee,' we should probably expect some proton deficit compared to HZE. At least some data favor such an assertion [29].

Some recent publications on the origin of spectral features in the ultrarelativistic range are of interest. In [39], arguments are presented indicating that the crossover to extragalactic CRs occurs at energies of 5×10^{17} eV. Another interesting hypothesis is discussed in [39]: that the foot (or ankle) is the intersection of fluxes of two independent extragalactic populations of UHECR particles. The foot is then to be

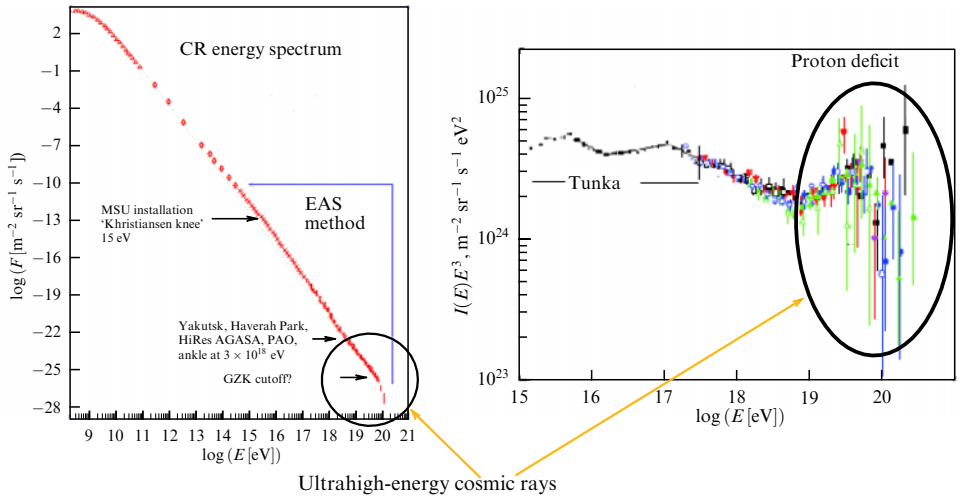

Figure 21. (Color online.) Proton deficit in the range beyond the knee [29].

explained either as a consequence of the propagation of extragalactic CRs or as a result of their interactions in their sources. The first possibility is ruled out by the composition data. A viable alternative is the photodecay of CR nuclei on background photons within the sources themselves, which can be either AGNs or gamma-ray bursts.

7.3 Exotic sources

We now consider some examples of exotic UHECR sources. The properties of the CR acceleration model in associations of O- and B-type stars at the stage of multiple supernova bursts are discussed in [174]. Assuming that supernovae are the most probable source of the CR energy in the Galaxy, the authors of [174] believe that, to explain the generation of high-energy ($E > 10^{14}$ eV) CRs, the inhomogeneous distribution of supernovae in the disk and the time correlation of their burst moments must be taken into account. Stellar winds of massive hot stars and supernovae flaring in the OB association blow out cavities filled with hot plasma in the interstellar medium. The size of the cavities can reach several hundred parsecs; they are surrounded by massive, slowly expanding shells. The maximum energy of accelerated particles is determined from the condition $E_{\max} \approx ZeB_0 l$, where Ze is the particle charge and B_0 is the magnetic field strength in the cavity of a scale l.

We emphasize that the maximum energy is proportional to Z. At energies not exceeding $E_{\max}$, acceleration occurs on separate SWs, and at energies exceeding $E_{\max}$, on ensembles of SWs and magnetic fields present in the cavity. An increase in the spectrum exponent with increasing energy leads to the enrichment of CRs in heavy elements (nuclei). The acceleration model in supernova associations allows qualitatively explaining the GCR spectrum in the energy range of 10^{15}–10^{18} eV. In this approach, the break in the energy spectrum is interpreted as a change in the acceleration mode.

On the other hand, a group of researchers [185] subjected the Fermi-type acceleration in astrophysical jets to a detailed theoretical analysis. The authors of [185] discuss DSA, second-order Fermi acceleration, and gradual shear acceleration. Special attention is given to recent progress in the field of viscous shear acceleration. The authors analyze the corresponding characteristic acceleration times and the resulting particle distributions; they also discuss the relation of these processes to the acceleration of charged particles in jets associated with AGNs, gamma-ray bursts, and microquasars. They show that multicomponent distributions of particles with power-law spectra are then likely to form.

Although the relations obtained in [185] are based on a simple model of test particles, which ignores any effects of a back reaction of the accelerated particles (for example, strong alterations in the SW, the kinetic energy of viscous dissipation, or significant SW deceleration), the authors of [185] believe that this approach still allows the amplitudes to be estimated within a reasonable order of magnitude in many interesting cases. Although there are different physical conditions in relativistic jets coming from AGNs, microquasars, and gamma-ray bursts, the analysis in [185] shows that Fermi-type acceleration processes provide a powerful and rather viable basis for explaining the origin of nonthermal particle distributions. In particular, due to the inverse scaling $t_{\rm acc} \propto 1/\lambda$, where $t_{\rm acc}$ is the characteristic acceleration time and λ is the transport diffusion path, shear acceleration is likely to become important at high energies and can therefore naturally lead to the appearance of at least a two-component energy distribution of particles.

Thus, relativistic jets generated by AGNs and gamma-ray bursts can be associated with very significant sources of acceleration of ultrahigh-energy particles. We have already mentioned important review article [172]; in addition, we note detailed paper [186] and also [187].

Another possibility of particle acceleration to ultrahigh energies, the acceleration in relativistic waves excited by explosions in the interstellar medium, is discussed in [188, 189]. As a generator of high-energy CRs, a surfatron mechanism for the acceleration of charged particles trapped by relativistic wave fronts is proposed there. The conditions making surfatron acceleration possible are discussed (see monograph [19] for more details). It is shown that, in plane and spherical relativistic waves, surf can accelerate CRs to ultrahigh energies (up to 10^{20} eV). Surfing in nonlinear Langmuir waves excited by strong electromagnetic radiation or powerful relativistic beams, as well as in strong SWs generated by relativistic jets or rapidly expanding spherical formations (fireballs), is discussed.

Other acceleration mechanisms under discussion include acceleration on a standing SW during the rotation of a neutron star with a powerful magnetic field ($\sim 10^{12}$ G). The maximum particle energy can then reach $(10^{17}$–$10^{18})Z$ eV, and the effective acceleration time, 10 years. Particle acceleration is also possible in SWs formed in galactic collisions. Such an event can occur at a rate of about once every 5×10^8 years; the maximum attainable energy in this case is estimated as $(3 \times 10^{19})Z$ eV. A similar estimate is also obtained for the process of acceleration by SWs in relativistic jets generated by AGNs. Approximately the same estimates are given by models wherein acceleration by SWs caused by the accretion of matter in galaxy clusters is discussed (see, e.g., [190]). The highest estimates (up to $\sim 10^{21}$ eV) can be obtained in the model of the cosmological origin of gamma-ray bursts. Even more exotic scenarios are also discussed, in which conventional particle acceleration is not required at all. In such scenarios, CRs arise as a result of the decay or annihilation of so-called topological defects such as cosmic strings, monopoles, and axions, which appeared in the first instants of the expansion of the Universe (see, e.g., [191, 192]).

8. Fermi mechanism: universal or dominant?

As noted in the Introduction, Fermi was the forerunner of the idea of stochastic acceleration on interstellar magnetic field inhomogeneities [13, 14]. On the other hand, by the mid-20th century, ground-based observations of CR intensity variations led to the discovery of SWs in circumsolar plasma (see, in particular, Section 2.4), where solar particles can be accelerated to relativistic energies (see Section 5.1). We chose the Fermi-type mechanism as the most natural and sufficiently general one for a magnetized plasma. Indeed, as is now established, SWs and particle acceleration occur in all plasma structures, from Earth's magnetosphere to the Sun's atmosphere, from the interplanetary medium to interstellar space, from supernovae to quasars, AGNs, etc. In any case, Fermi-type acceleration processes offer a powerful and viable basis (or at least an explanatory framework) for the origin of nonthermal particle distributions in these sources. It is appropriate to formulate our two main postulates here: first, what exactly is meant by stochastic acceleration, and second, what do we mean by saying that 'this mechanism can be dominant.'

8.1 Basic postulates

(1) By the 'Fermi-type stochastic acceleration mechanism,' we mean acceleration on SWs, which obviously occurs everywhere from Earth's magnetosphere to the Sun (flares) and from the solar wind (including CMEs) to supernovae and quasars, etc.

(2) In the background of a possible simultaneous action of two or more acceleration mechanisms in the same object (for example, in a solar flare), the parameters of the distribution function of the accelerated particles are mainly determined by the action of the Fermi mechanism. In the framework of this review, this amounts to the formation of power-law spectra and enrichment with heavy particles.

We discuss these possibilities in greater detail.

8.2 Development of the Fermi model

As is known, the Fermi hypothesis was mainly developed along two lines (see, e.g., books [18, 64] for detailed reviews and references). In a process called *first-order* Fermi acceleration, two magnetic mirrors (clouds) are continuously moving toward each other, such that the particles repeatedly oscillate back and forth, regularly increasing their energy with each reflection. The energy increases in proportion to the ratio U/v, where U is the speed of the cloud and v is the speed of the particle. This process is sometimes simply called acceleration on an SW (see, e.g., [144]). An important role is played here by the degree of plasma compression σ in the SW (in [144], σ was taken in the range of ~ 1.6–3.0).

In the case of *second-order* Fermi acceleration (*stochastic* acceleration proper), the clouds move in random directions. In 'head-on' collisions, particles acquire energy, and in 'overtaking' collisions, lose energy. But because of the difference in the relative speeds U and v, in both the first and second cases, the probability of head-on collisions is higher than the probability of overtaking ones, which eventually results in a net increase in energy, but this time proportional to U^2/v^2, more precisely, to $(u_A/v)^2$, where u_A is the Alfven velocity in the plasma.

Modern views on the kinematics of particle reflection during Fermi-type acceleration [13, 14] and the geometry of the corresponding magnetic configurations (magnetic clouds) are illustrated in Figs 22. The initial 'push' to start energizing the particle can occur on a curved section of the field line and/or at the reflection points.

Fermi's original idea of CR acceleration by interstellar clouds has undergone major changes over time, but both mechanisms, first and second order, have been greatly developed and preserve their importance in astrophysics. The first-order mechanism can operate, in particular, between oppositely directed MHD pulses [193] or accreting astrophysical flows (see, e.g., [190, 194]). But the most efficient configuration in which it works is apparently the *shock wave*.

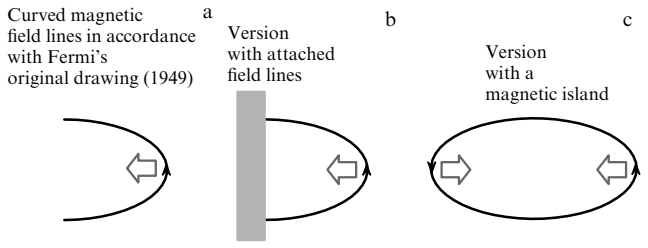

Figure 22. Kinematics of particle reflection and geometry of the Fermi mechanism operation according to modern concepts (from Panasyuk's talk on May 22, 2019).

8.3 Physical justification

The modern physical justification of the Fermi mechanism [13, 14] came almost 30 years after its inception: it was shown in [195–201] that the most efficient configuration in which the mechanism actually works is a *shock wave*. In Russian studies, the corresponding acceleration mechanism on SWs is called 'regular' [195, 200, 201], while in the English literature this process is more often referred to as DSA (diffusive shock acceleration). The idea is that the acceleration occurs near the SW front (Fig. 23), with particles scattered on magnetic inhomogeneities (wave turbulence) of the plasma and the accelerated particles temporarily retained near the SW front.

Scattering and acceleration of particles occur during the passage of a shock front (see Fig. 23). The difference between plasma speeds at the front, $\Delta V = V_s - V$, is the source of MHD energy for the acceleration. In other words, the energy of the accelerated particles is drawn from the SW energy, and the turbulence before and behind the front keeps the particles close to the front until the moment of their escape.

8.4 Features of SW acceleration

The most characteristic features of acceleration on SWs are as follows. In the ideal case of an infinite plane wave in stationary conditions, the differential particle intensity dJ/dE can be described by the power-law function $dJ/dE \sim E^{-\gamma}$, where γ is determined by the SW compression ratio σ: $\gamma = (\sigma + 2)/(\sigma - 1)$ (see, e.g., [191]). This means that the spectrum of accelerated particles under the action of the regular mechanism turns out to be independent of the parameters of the medium in which the SW propagates. The simple form of the dependence of the spectrum shape on the SW parameters is an undoubted advantage of the DSA model. This 'universality' of the proposed mechanism was noted by Krymskii as early as 1977 [195]. In strong SWs, the compression degree lies in the range $\sigma = 3$–4 [201], and hence the spectral exponent of accelerated particles exactly corresponds to that observed in most of the GCRs and relativistic electrons in supernova remnants. On the whole, the spectra of accelerated particles and the parameters of SWs seem to be in good agreement with each other.

We note, however, that DSA is a rather slow process (see, e.g., [202]). A particle acquiring the energy $pv = 2E_k$ requires N^2 scatterings with energy changing at the front crossing,

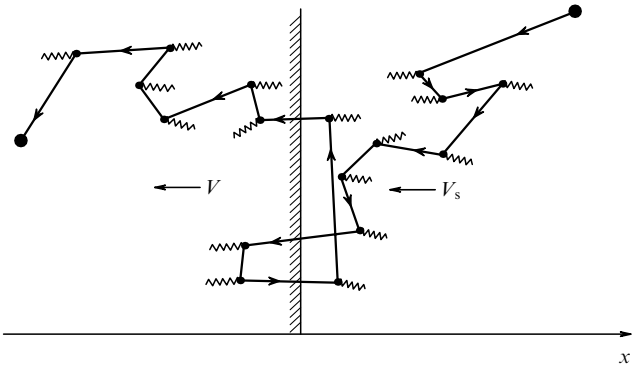

Figure 23. Schematic of particle confinement near a SW front for stochastic Fermi acceleration: DSA model [202].

with $N = v/\Delta V$, where E_k is the kinetic energy of the particle and p and v are its momentum and speed. In addition, for effective acceleration, the condition $v \gg V$ must be satisfied (the injection problem); otherwise, particles would simply escape from the upstream region through the front to the downstream region.

In what follows in this review, our phenomenological approach to Fermi acceleration processes notwithstanding, it would be useful to give simple estimates of other characteristic parameters of Fermi-type acceleration, for example, the energy gain rate α and the total acceleration time T. Nonetheless, it is quite difficult to make such estimates in view of the wide variety of plasma media in astrophysics and the ensuing huge variety of the 'initial' and 'boundary' conditions for acceleration. As an example, we present the parameters of media such as the solar wind and interstellar gas in the Galaxy. In the first case, the density of particles in the medium is ~ 1 cm^{-3}, the magnetic field strength is ~ 1 nT, and the Mach number is ~ 5; in the second case, the respective parameters are $\sim 10^{-3}$ cm^{-3}, $\sim 10^{-2}$ nT, and ~ 100 [29]. A separate problem must actually be solved for each chosen plasma medium, and each astrophysical situation is unique from the standpoint of particle acceleration.

A thorough comparative analysis of SW acceleration (the DSA model) and stochastic acceleration processes was given in [203] from a theoretical standpoint. It was shown that SW acceleration and stochastic acceleration have much in common. The SW front-crossing rate in the DSA mechanism is equivalent to the particle scattering rate under stochastic acceleration. As noted in [203], the 'magic' of the SW acceleration theory is that the parameters α (acceleration rate) and T (acceleration time) are related such that their product αT depends only on the plasma compression degree σ in the SW. Astrophysical SWs are typically strong: their degree of compression ensures the formation of the observed power-law spectra of accelerated particles.

We note that two variants of the implementation of the Fermi mechanism apparently operate in the NES, as shown in Fig. 22a, b. Another important point is that the energy of an accelerated particle then increases in proportion to its charge, $E \sim Z$. Any physical mechanism responsible for the particle injector must ensure the particle flux relation Fe/H > O/H > C/H > He/H on inner magnetic shells (at distances less than $2R_E$ in the equatorial plane) for $E > 1$ MeV [29]. The variant shown in Fig. 22c is apparently realized in the interplanetary plasma.

9. Summing up...

Stating the *dominant* role of the considered Fermi mechanism means that, in the background of the possible simultaneous action of two or more acceleration mechanisms (for example, in a solar flare), the parameters of the distribution function of accelerated particles are mainly determined by the action of the stochastic Fermi mechanism. In the context of this review, this corresponds to the formation of power-law spectra and enrichment in heavy particles, although the latter effect is far from evident.

Before summarizing the general results of our consideration of the problem posed in the title, we note the following. Many researchers agree that there are two important aspects (or levels of consideration) in the problem of charged particle acceleration in space: global (MHD, or macroprocesses) and local (microprocesses).

9.1 Two levels of the acceleration problem

The first aspect includes the interaction of accelerated particles with large-scale MHD structures, for example, magnetic clouds in the Galaxy. The second case relates to microprocesses that develop on relatively small space–time scales, including in solar flares (see, e.g., [24, 204]). Both aspects are closely related to each other and have already been widely covered in the literature (see, e.g., [25, 27, 201]). The authors of [201] noted that all variants of statistical mechanisms have a common physical content. Fast particles and scattering centers are similar to two different gases. The scattering centers are macroscopic volumes of plasma, and hence they can be assigned an infinitely high temperature. Their thermal contact with fast particles via scattering leads to the transfer of energy from scattering centers to particles, which means accelerating the particles. In other words, the acceleration process acts here as an analogue of ordinary heating in collisional plasmas. Such an analogy has a rather general physical character: heating in collisional plasma corresponds to particle acceleration in collisionless plasma. A derivation and detailed discussion of the fundamental equations for the macroscopic dynamics of space plasma can be found in review [205], with nonthermal particles, fluctuating electromagnetic fields, and neutral atoms taken into account.

An approach similar to [201] was recently developed in [18, 206]. The proposal in [206], in particular, was to divide CRs into external and internal relative to the object under consideration and to study them separately (interplanetary CRs, magnetospheric CRs, etc.). It was also proposed in [206] to separately consider different types of stellar CRs. This is similar to the previous proposal [207] regarding the possible greater role of dwarf stars in explaining some anomalies in the spectra of protons and helium nuclei found by the international PAMELA experiment (see, e.g., [208]). In particular, it was found that the spectra of particles of these two types have different shapes and cannot be reliably described by a single power law. These data challenge the current concept of CR acceleration in supernova remnants and their subsequent diffusion in the Galaxy. Explaining the spectral features obtained in observations with the PAMELA orbital spectrometer requires postulating more complex processes of CR acceleration and transfer.

9.2 Some prospects for the study of cosmic rays

In speaking about the prospects for further CR studies, we first note that the acceleration of particles in cosmic plasma is generally recognized as a universal phenomenon in the Universe (see, e.g., monograph [18]). It also follows from our consideration that the most important research problems reside at opposite 'ends' of the CR spectrum. For example, the beginning of acceleration starting with the thermal distribution of particles brings about the injection problem; after that, the particle must overcome the Dreicer field [209], and so on. This is especially true for acceleration in solar flares (see [204]). In the range of ultrahigh energies, the search for the sources of such particles is underway, because the Hillas rule, for example, forbids the existence of Zevatrons — particles with energy $E > 3 \times 10^{20}$ eV.

The idea of a possible contribution from nearby sources directly echoes the results of the ATIC experiment (see Section 6) and the results of an analysis of data obtained aboard the Kepler SC (see, e.g., [210, 211]) in observations of superflares on other solar-type stars. An energy of up to 10^{35}–10^{36} erg is released in such events.

One of the arguments against the 'universality' of the Fermi acceleration and the abundance of HZE particles in CR composition amounts to taking the metallicity of stars into account. In accordance with the view expressed in [46], the presence of a large number of HZE particles in the CR composition seems unlikely from the standpoint of the metallicity of stars. As regards the chemical composition of CRs, it is noted in [46], in particular, that, from the astrophysical standpoint, the presence of a large number of primary heavy nuclei seems less probable than the (mostly) proton composition. This conclusion is substantiated by the fact that the presence of a large number of HZE particles requires some mechanisms for increasing the metallicity of the injected material in sources by several orders of magnitude compared to the maximum known stellar metallicity. The argument related to more efficient HZE acceleration leads to the requirement for a sharp and experimentally unobserved jump [46] in both the composition and total flux of CRs at energies corresponding to the maximum energies of accelerated protons. At present, according to [46], the question of the chemical composition of UHECRs remains open.

Unfortunately, observational data for all considered CR sources (from SEPs to quasars, AGNs, relativistic jets, etc.) are either insufficiently accurate or contradictory. An obvious drawback of any attempt at interpretation is that it is universally difficult to 'forego' the model of the relevant phenomenon or event.

As regards GCRs (in the energy range above the break, or knee), and especially in the UHECR range, models of nuclear interaction (elementary events) at energies as high as $E > 3 \times 10^{18}$ eV acquire particular importance. Astrophysical research in the field of ultrahigh energies requires making certain assumptions about hadronic interactions. Such assumptions are implemented in phenomenological models, whose parameters are determined from accelerator data. As noted in [212], this introduces uncertainty into the interpretation of the experimental results obtained in UHECR studies, because some elements of the model have to be extrapolated outside the area in which they were verified.

Meanwhile, according to the estimates in [213], no reliable observational data can exist on the composition of CRs with energies above 10^{19} eV. This situation will be preserved until the inconsistencies between the models of hadron interactions and observational data on EAS development are eliminated, because different models lead to different chemical compositions. Another possibility not to be ruled out is the anisotropy of the chemical composition at the highest energies, with the deviations of particles being already small and the sources few; individual nearby sources can then form different patterns in CR observations from the northern parts of the sky (TA) and from southern sources (PAO). We may be observing this in the spectra [213].

For several decades, UHECR physics has remained one of the most exciting areas at the intersection of astrophysics and elementary particle physics [46]. Despite significant experimental progress, we can still say little about the origin of particles with energies $E > 10^{19}$ eV. Only a few models of particle acceleration in astrophysical sources can simultaneously satisfy the requirements imposed on the physical conditions in these space accelerators. In addition, acceleration models must obey a strict lower bound on the source density. Such a constraint was obtained recently based on the absence of clusters of arrival directions [46]. According to [46], in results from studies of the chemical composition of primary particles with such energies, systematic errors apparently dominate over contributions due to physical effects. The physical cause underlying the systematic difference in determining the primary particle energy by different methods remains unknown.

Some indications of possible manifestations of the 'new physics' in CRs deserve close attention (see, e.g., [182, 214]). According to [182], photons can transform into axions and back in the magnetic fields of various astrophysical objects, including active galaxies, galaxy clusters, intergalactic space, and the Milky Way. This may be an explanation for candidate ultrahigh-energy neutral particles ($E > 10^{18}$ eV) from distant objects such as BL Lac, which may have been observed by the HiRes collaboration (High Resolution Fly's Eye experiment) [215]. The decay of hypothetical axions with the same mass and connectivity can also explain photons with an energy of the order of 1 TeV (10^{12} eV) detected from distant blazars.

As regards solar CRs, their elemental composition and charge state will apparently remain the subject of dedicated theoretical (model) and experimental studies for the foreseeable future. In particular, the systematic correlation of spectra and elemental abundance provides a new perspective both for the 'injection problem' [169] in the selection of ions by SWs and for the physics of SEP acceleration and transport.

To understand the features of SEP acceleration, especially at the initial stage of a solar flare, so-called blow-up regimes are of great interest (see, e.g., [216] and references therein). Blow-up regimes were discovered in the 1970s in studies of the problem of controlled thermonuclear fusion when solving the heat conduction equation for the combustion process [217]. In the blow-up mode, a physical quantity (energy, temperature, etc.) increases without bound in some region of space.

In [216], the nature of the observed localization of hot flare plasma in the form of small-scale structures was investigated and plasma energization was related to magnetic tube waists. The waists are in turn caused by the plasma instability during the flow of an electric current or the passage of a shock. Dynamic magnetic traps then form in which charged particles are accelerated at the early phase of the flare by the Fermi mechanism. In the case of converging waists, which serve as magnetic mirrors for charged particles, the regular first-order Fermi acceleration mechanism becomes efficient. In a collapsing trap, the longitudinal component of the particle momentum $p_{||}$ increases [15, 218], and the trapped plasma is heated in accordance with a hyperbolic law [219]. Thus, as a result of magnetic compression, the charged particles are accelerated and the plasma is heated. The observed rapid heating reflects the nonlinear nature of the magnetic field amplification in the waist. Heating of the primary source in the peaking mode is accompanied by a simultaneous filamentation of the tube and a decrease in the filling factor. This results in a two-stage nature of the gasdynamic response of the solar chromosphere.

In addition, understanding the features of SEP, ACR, and GCR acceleration is also important in solving some related problems, such as protection against radiation hazard (see, e.g., [220]) and a number of problems in solar-terrestrial physics and solar-terrestrial relations (see, e.g., [221]).

9.3 Modern view of the injection problem

As we have noted more than once, a difficulty facing the theory of acceleration is rooted in the injection problem, which is directly related to the problem of the nuclear composition of primary CRs. Naturally, researchers are

seeking new methods to tackle this problem. The so-called particle-in-cell (PIC) method has turned out to be one of the most fruitful and powerful methods for this purpose. It has been known for a relatively long time, since the mid-20th century. In the early 1990s, at the junction of laser physics and plasma physics, a new actively developing field appeared: the physics of the interaction of high-power laser radiation with matter. But the PIC method, well known and well developed by that time, was largely ignored by researchers working in the new field. The prevailing belief was that the method was not good enough for their tasks, because of its low accuracy. The attitude towards the PIC method changed dramatically after paper [222] appeared in 2004.

When applied to plasma and accelerator problems, the PIC method amounts to modeling plasma by particles in cells. In a number of studies carried out over the past decade [223–226], it has been shown that the most consistent solution to the complex injection problem can be obtained on the basis of direct plasma simulation using the PIC method. For example, the results of a hybrid PIC simulation of SWs in space plasma with an admixture of heavy, weakly charged ions are presented in [223]. The simulation relied on the three-dimensional hybrid code proposed previously in [225] of the second order of accuracy with respect to time and with exactly maintained zero divergence of the magnetic field.

The first calculations of ion acceleration by the DSA mechanism on nonrelativistic SWs were presented in [224]. Using hybrid modeling (with kinetic ions and fluid electrons), the thermalization, injection, and acceleration of ions with different mass-to-charge ratios A/Z were studied in nonrelativistic collisionless SWs. Particles with large A/Z values were shown to have enhanced nonthermal tails compared to protons, which quantitatively agrees with the observed GCR chemistry, the maximum length of nonthermal tails being $\propto E/Z$.

The results of a hybrid simulation of the diffusion acceleration of particles in collisionless SWs with an admixture of elements heavier than hydrogen were presented in [226]. The injection of various ions into the acceleration process, the efficiency of acceleration, and the transport of energetic particles and their resulting energy spectra are considered. The results are presented for SWs with parameters characteristic of plasma media such as the solar wind, supernova remnants, and galaxy clusters. Simulations showed that, for all types of ions, three adjacent spatial regions with different diffusion regimes can be distinguished. It was shown, in particular, that for the most energetic protons, the quasilinear theory is valid in the entire simulation region, while for heavy, weakly charged ions, the region of Bohm diffusion is almost absent. The boundaries of the regions are marked by a below-threshold decrease in the level of resonant fluctuations. The results of a hybrid modeling of particle acceleration on collisionless SWs were recently generalized in [227]. One of the most interesting results in [227] consists in identifying the mechanism of preferential acceleration of heavy ions in backward SWs from supernova remnants. The effect that heavy ions exert on the injection of protons into the first-order Fermi acceleration process was also studied.

Recently, the enrichment in ^{3}He ions, which is often observed in pulsed SEP events, was simulated in [228]. A variant of the PIC method with 1.5 measurements was used for the simulation. The interaction of an electron beam with plasma was simulated that generates electron and ion cyclotron waves (cyclotron waves for protons and ^{4}He ions). The dispersion of these waves depends on the particle magnetization $\alpha = \omega_{pe}/\Omega_{ce}$ (where ω_{pe} is the plasma or Langmuir frequency of electrons and Ω_{ce} is the cyclotron frequency of electrons), as well as on the ratio of electron and proton temperatures $\tau = T_e/T_p$. Background particles such as ^{3}He and ^{4}He are in resonance with the excited cyclotron waves and experience selective heating or acceleration. The specific resonance modes for the ^{3}He ions lead to a higher acceleration rate than that of the ^{4}He ions. It is noted in [228] that the results of this simulation open up the possibility of understanding the enrichment of the solar wind with heavy ions.

10. Conclusion

The variety of existing theories and models of particle acceleration in space is evidence of the unsolved status of this problem in general. The data on the nuclear composition of accelerated particles obtained in numerous experiments can testify in favor of the global nature of the Fermi-type stochastic acceleration mechanism inherent in various astrophysical objects. This mechanism can also be dominant among others. Nevertheless, it seems obvious that a number of experimental observations are inconsistent with this conclusion. In some space objects, a hierarchy of accelerating mechanisms can possibly exist, with the preliminary acceleration by one mechanism followed by other mechanisms switching on sequentially or alternately. This approach is quite natural in view of the wide variety of the 'initial' and 'boundary' conditions for the acceleration of charged particles in space. New experiments and new model and theoretical studies are needed, but observational data are still of major significance.

We note, however, that energetic particles are not a by-product but the most important component of the Universe [229]. Energetic particles are the key to understanding energy conversion and energy transfer in explosive situations in astrophysical plasmas, as well as in more gradual and long-lived processes in those structures that, for example, exhibit strong gradients and turbulence.

More than 100 years have passed since the discovery of GCRs, and about 80 years since the first reliable registration of SEPs, which was proof of the fundamental possibility of particle acceleration in stellar atmospheres or near stars. However, most of the problems related to the acceleration mechanisms are still unresolved. At the same time, CRs remain at the forefront of astrophysical research. As Cocconi noted back in 1959, "Ultimately, if we want to stay on solid ground, we can be sure of only two generators of cosmic rays: the Sun and the Universe" [230].

This review is based on a plenary topical talk jointly presented by the two authors at the regular 36th National Conference on Cosmic Rays_2020 (RCRC_2020) (http://rcrc2020.sinp.msu.ru). This talk, which was given on September 28, 2020, turned out to be the last public talk by Panasyuk, who passed away on November 3, 2020 [231].

L I M expresses deep gratitude to S V Troitsky (Institute for Nuclear Research, Russian Academy of Sciences) for a number of important references, much advice, and many remarks, and to V G Yanke (Pushkov Institute of Terrestrial Magnetism, the Ionosphere, and Radio Wave Propagation, Russian Academy of Sciences) for their help in preparing the manuscript. A number of comments and suggestions from the

referee proved to be very valuable and significantly influenced the content of the review.

References

1. Hess V F *Phys. Z.* **13** 1084 (1912)
2. Dorman I V *Kosmicheskie Luchi* (Cosmic Rays) (Moscow: Nauka, 1981)
3. Dorman I V, Dorman L I *Adv. Space Res.* **53** 1388 (2014)
4. Swann W F G *Phys. Rev.* **43** 217 (1933)
5. Lange I, Forbush S E *Terr. Magn. Atmos. Electr.* **47** 331 (1942)
6. Forbush S E *Phys. Rev.* **70** 771 (1946)
7. Adams N *Philos. Mag. 7* **41** 503 (1950)
8. Forbush S E, Stinchcomb, T B, Schein M *Phys. Rev.* **79** 501 (1950)
9. Krasil'nikov D D, Kuz'min A I, Shafer Yu G "Variatsii intensivnosti kosmicheskikh luchei" ("Cosmic ray intensity variations") *Tr. Yakutskogo Filiala Akad. Nauk SSSR Ser. Fiz.* (1) 41 (1955)
10. Miroshnichenko L I *Phys. Usp.* **61** 323 (2018); *Usp. Fiz. Nauk* **188** 345 (2018)
11. Swann W F G, in *Proc. of the 6th Intern. Cosmic Ray Conf., July 1959, Moscow, USSR* Vol. 3 (Ed. S I Syrovatsky) (Moscow, 1960) p. 167
12. Baade W, Zwicky F *Proc. Natl. Acad. Sci. USA* **20** 259 (1934)
13. Fermi E *Phys. Rev.* **75** 1169 (1949)
14. Fermi E *Astrophys. J.* **119** 1 (1954)
15. Ginzburg V L, Syrovatskii S I *The Origin of Cosmic Rays* (Oxford: Pergamon Press, 1964); Translated from Russian: *Proiskhozhdenie Kosmicheskikh Luchei* (Moscow: Izd. AN SSSR, 1963)
16. Toptygin I N *Cosmic Rays in Interplanetary Magnetic Fields* (Dordrecht: D. Reidel, 1985); Translated from Russian: *Kosmicheskie Luchi v Mezhplanetnykh Magnitnykh Polyakh* (Moscow: Nauka, 1983)
17. Berezinskii V S et al. *Astrophysics of Cosmic Rays* (Ed. V L Ginzburg) (Amsterdam: North-Holland, 1990); Translated from Russian: *Astrofizika Kosmicheskikh Luchei* (Ed. V L Ginzburg) (Moscow: Nauka, 1990)
18. Dorman L I *Cosmic Ray Interactions, Propagation, and Acceleration in Space Plasmas* (Dordrecht: Springer, 2006)
19. Kichigin G N, Strokin N A *Protsessy Energovydeleniya v Kosmicheskoi Plazme* (Energy Release Processes in Space Plasma) (Irkutsk: Izd. Irkutskogo Gos. Tekh. Univ., 2007)
20. Ginzburg V L, Syrovatskii S I *Sov. Phys. Usp.* **3** 504 (1961); *Usp. Fiz. Nauk* **71** 411 (1960); *Sov. Phys. Usp.* **9** 223 (1966); *Usp. Fiz. Nauk* **88** 485 (1966)
21. Somov B V, Syrovatskii S I *Sov. Phys. Usp.* **19** 813 (1976); *Usp. Fiz. Nauk* **120** 217 (1976)
22. Syrovatskii S I *Annu. Rev. Astron. Astrophys.* **19** 163 (1981)
23. Antonova E E et al. *Uskoritel'nye Mekhanizmy v Kosmose* (Accelerator Mechanisms in Space) (Moscow: Izd. MGU, 1988) Textbook
24. Miller J A et al. *J. Geophys. Res.* **102** (A7) 14631 (1997)
25. Miroshnichenko L I *Solar Cosmic Rays* (Dordrecht: Kluwer Acad. Publ., 2001)
26. Miroshnichenko L I *Izv. Ross. Akad. Nauk. Fiz.* **67** 400 (2003)
27. Miroshnichenko L *Solar Cosmic Rays*: *Fundamentals and Applications* 2nd ed. (Cham: Springer Intern. Publ., 2015)
28. Panasyuk M I *Stranniki Vselennoi ili Ekho Bol'shogo Vzryva* (Wanderers of the Universe or the Echo of the Big Bang) (Fryazino: Vek 2, 2005)
29. Panasyuk M I *Radioaktivnaya Vselennaya* (Radioactive Universe) (Fryazino: Vek 2, 2019)
30. Zelenyi L M et al. *Phys. Usp.* **53** 933 (2010); *Usp. Fiz. Nauk* **180** 973 (2010)
31. Frank A G *Phys. Usp.* **53** 941 (2010); *Usp. Fiz. Nauk* **180** 982 (2010)
32. Kuznetsov V D *Phys. Usp.* **53** 947 (2010); *Usp. Fiz. Nauk* **180** 988 (2010)
33. Somov B V *Phys. Usp.* **53** 954 (2010); *Usp. Fiz. Nauk* **180** 977 (2010)
34. Ptuskin V S *Phys. Usp.* **53** 958 (2010); *Usp. Fiz. Nauk* **180** 1000 (2010)
35. Dorman L I *Phys. Usp.* **53** 496 (2010); *Usp. Fiz. Nauk* **180** 519 (2010)
36. Zelenyi L M et al. *Phys. Usp.* **56** 347 (2013); *Usp. Fiz. Nauk* **183** 365 (2013)
37. Zelenyi L M et al. *Phys. Usp.* **59** 1057 (2016); *Usp. Fiz. Nauk* **186** 1153 (2016)
38. de Nolfo G A et al. *Adv. Space Res.* **38** 1558 (2006)
39. Kachelrieß M, Semikoz D V *Prog. Part. Nucl. Phys.* **109** 103710 (2019); arXiv:1904.08160
40. Miroshnichenko L I, Petrov V M *Dinamika Radiatsionnykh Uslovii v Kosmose* (Dynamics of Radiation Conditions in Space) (Moscow: Energoatomizdat, 1985)
41. Miroshnichenko L I, in *Space Weather Effects on Humans*: *in Space and on Earth. Proc. of the Intern. Conf. Space Research Institute, Moscow, Russia, June 4–8, 2012. Mezhdunarodnaya Konf. Vliyanie Kosmicheskoi Pogody na Cheloveka v Kosmose i na Zemle, 4–8 Iyunya 2012, IKI RAN, Moscow, Russia. Trudy* Vol. 1 (Eds A I Grigor'ev, L M Zelenyi) (Moscow: Space Research Institute, 2013) p. 110–136; Grigor'ev A I, Zelenyi L M (Eds) *Space Weather Effects on Humans*: *in Space and on Earth. Proc. of the Intern. Conf. Space Research Institute, Moscow, Russia, June 4–8, 2012. Mezhdunarodnaya Konf. Vliyanie Kosmicheskoi Pogody na Cheloveka v Kosmose i na Zemle, 4–8 Iyunya 2012, IKI RAN, Moscow, Russia. Trudy* Vol. 1 (Moscow: Space Research Institute, 2013) http://www.iki.rssi.ru/books/2013breus1.pdf; Grigor'ev A I, Zelenyi L M (Eds) *Space Weather Effects on Humans*: *in Space and on Earth. Proc. of the Intern. Conf. Space Research Institute, Moscow, Russia, June 4–8, 2012. Mezhdunarodnaya Konf. Vliyanie Kosmicheskoi Pogody na Cheloveka v Kosmose i na Zemle, 4–8 Iyunya 2012, IKI RAN, Moscow, Russia. Trudy* Vol. 2 (Moscow: Space Research Institute, 2013) http://www.iki.rssi.ru/books/2013breus2.pdf
42. Panasyuk M et al., in *Extreme Events in Geospace*: *Origins, Predictability, and Consequences* (Ed. N Buzulukova) (Amsterdam: Elsevier ST Books, 2018) p. 349, https://doi.org/10.1016/B978-0-12-812700-1.00013-3
43. Garipov G K et al. *Cosmic Res.* **58** 242 (2020); *Kosmicheskie Issled.* **58** 276 (2020)
44. Hillas A M *Annu. Rev. Astron. Astrophys.* **22** 425 (1984)
45. Ptitsyna K V, Troitsky S V *Phys. Usp.* **53** 691 (2010); *Usp. Fiz. Nauk* **180** 723 (2010)
46. Troitsky S V *Phys. Usp.* **56** 304 (2013); *Usp. Fiz. Nauk* **183** 323 (2013)
47. Shea M A, Smart D F *Space Sci. Rev.* **93** 187 (2000)
48. Cornwall J M, in *Ion Acceleration in the Magnetosphere and Ionosphere* (Geophysical Monograph, Vol. 38, Eds T Chang et al.) (Washington, DC: Amer. Geophys. Union, 1986) p. 3
49. Bryant D A *Electron Acceleration in the Aurora and Beyond* (Bristol: Inst. of Physics Publ., 1999)
50. Möbius E *Astrophys. J. Suppl.* **90** 521 (1994)
51. Burgess D, Möbius E, Scholer M *Space Sci. Rev.* **173** 5 (2012)
52. Balogh A, Treumann R A *Physics of Collisionless Shocks. Space Plasma Shock Waves* (ISSI Scientific Report Ser., Vol. 12) (New York: Springer, 2013) https://doi.org/10.1007/978-1-4614-6099-2
53. Millan R M, Baker D N *Space Sci. Rev.* **173** 103 (2012)
54. Thorne R M et al. *Nature* **504** 411 (2013)
55. Demekhov A G et al. *Geophys. Res. Lett.* **47** (6) e2020GL086958 (2020)
56. Murphy K R et al. *Geophys. Res. Lett.* **45** 3783 (2018)
57. Patel M et al. *Geophys. Res. Lett.* **46** 7222 (2019)
58. Claudepierre S G et al. *Geophys. Res. Lett.* **47** e2019GL086056 (2020)
59. Birn J, Hesse M, Schindler K *J. Geophys. Res.* **101** 12939 (1996)
60. Birn J et al. *J. Geophys. Res.* **102** 2325 (1997)
61. Birn J et al. *J. Geophys. Res.* **103** 9235 (1998)
62. Birn J et al. *Space Sci. Rev.* **173** 49 (2012)
63. Hones E W (Jr.) *J. Geophys. Res.* **82** 5633 (1977)
64. Priest E, Forbes T *Magnetic Reconnection*: *MHD Theory and Applications* (Cambridge: Cambridge Univ. Press, 2000); Translated into Russian: *Magnitnoe Peresoedinenie*: *Magnitogidrodinamicheskaya Teoriya i Prilozheniya* (Moscow: Fizmatlit, 2005)
65. Priest E R *Solar Phys.* **289** 3579 (2014)
66. Parker E N *J. Geophys. Res.* **65** 3117 (1960)
67. Tverskoy B A *Geomagn. Aeron.* **4** 351 (1964)
68. Fälthammar C-G *J. Geophys. Res.* **70** 2503 (1965)
69. Tverskoy B A *Geomagn. Aeron.* **5** 617 (1965)
70. Tverskoy B A *Dinamika Radiatsionnykh Poyasov Zemli* (Dynamics of the Earth's Radiation Belts) (Moscow: Nauka, 1968)
71. Tverskoy B A *Rev. Geophys.* **7** 219 (1969)
72. Tverskoy B A *Rev. Geophys.* **7** 219 (1969); Translated into Russian: Tverskoy B A, in *Fizika Magnitosfery* (Eds D J Williams, G D Mead) (Moscow: Mir, 1972) p. 278

73. Bakhareva M F, Lomonosov V N, Tverskoy B A *Izv. Akad. Nauk SSSR. Ser. Fiz.* **34** 2313 (1970)
74. Bakhareva M F, Lomonosov V N, Tverskoi B A *Sov. Phys. JETP* **32** 1086 (1971); *Zh. Eksp. Teor. Fiz.* **59** 2003 (1970)
75. Walt M, in *Particles and Fields in the Magnetosphere. Proc. of a Symp., Univ. of California, Santa Barbara, CA, USA, August 4 – 15, 1969* (Astrophysics and Space Science Library, Vol. 17, Ed. B M McCormack) (Dordrecht: D. Reidel Publ. Co., 1970) p. 410
76. Walt M *Space Sci. Rev.* **12** 446 (1971)
77. Shelley E G, Johnson R G, Sharp R D *J. Geophys. Res.* **77** 6104 (1972)
78. Shelley E G, Johnson R G, Sharp R D, in *Magnetospheric Physics. Proc. of the Advanced Summer Institute, Sheffield, UK, August 1973* (Astrophysics and Space Science Library, Vol. 44, Ed. B M McCormac) (Dordrecht: D. Reidel, 1974) p. 135
79. Shelley E G *Space Sci. Rev.* **23** 465 (1979)
80. Lennartsson W *Phys. Scr.* **36** 367 (1987)
81. Spjeldvik W N, Fritz T A *J. Geophys. Res.* **83** 1583 (1978)
82. Alfvén H *Tellus* **11** 106 (1959)
83. Panasyuk M I, in *Proc. of the 23rd Intern. Cosmic Ray Conf., Calgary, Alberta, Canada, 19–30 July, 1993. Invited, Rapporteur and Highlight Papers* (Eds D A Leahy, R B Hicks, D Venkatesan) (Singapore: World Scientific, 1994) p. 455
84. Panasyuk M I, in *Matter, Antimatter, and Dark Matter. Proc. of the 2nd Intern. Workshop, Trento, Italy, 29–30 October 2001* (Eds R Battiston, B Bertucci) (River Edge, NJ: World Scientific, 2002) p. 117
85. Panasyuk M I, in *Model' Kosmosa* (Space Model) Vol. 1, 8th ed. (Ed. M I Panasyuk) (Moscow: KDU, 2007) p. 96
86. Grigorov N L et al. *Geophys. Res. Lett.* **18** 1959 (1991)
87. Bobrovskaya V V et al., in *Proc. of the 23rd Intern. Cosmic Ray Conf., Calgary, Alberta, Canada, 19–30 July, 1993. Contributed Papers* Vol. 3 (Calgary: Univ. of Calgary, 1993) p. 432
88. Bobrovskaya V V et al. *Izv. Ross. Akad. Nauk. Ser. Fiz.* **57** (7) 62 (1993)
89. Birn J et al. *Space Sci. Rev.* **173** 49 (2012)
90. Kovtyukh A S *Cosmic Res.* **39** 527 (2001); *Kosmicheskie Issled.* **39** 563 (2001)
91. Daglis I A *Space Sci. Rev.* **124** 183 (2006)
92. Kovtyukh A S, in *Model' Kosmosa* (Space Model) Vol. 1, 8th ed. (Ed. M I Panasyuk) (Moscow: KDU, 2007) p. 482
93. Dessler A J, Parker E N *J. Geophys. Res.* **64** 2239 (1959)
94. Sckopke N *J. Geophys. Res.* **71** 3125 (1966)
95. Sckopke N *Cosmic Electrodyn.* **3** 330 (1972)
96. Liemohn M W *J. Geophys. Res.* **108** 1251 (2003)
97. Kozyra J U, Liemohn M W *Space Sci. Rev.* **109** 105 (2003)
98. Vasyliūnas V M *Ann. Geophys.* **24** 1085 (2006)
99. Tverskoy B A *Osnovy Teoreticheskoi Kosmofiziki. Izbrannye Trudy* (Fundamentals of Theoretical Cosmophysics. Selected Works) (Comp. M F Bakhareva et al.) (Moscow: Editorial URSS, 2004)
100. Gloeckler G, Hamilton D C *Phys. Scr.* **1987** (T18) 73 (1987)
101. Klecker B, in *21st European Cosmic Ray Symp., 9–12 September 2008 Košice, Slovakia* (Košice: Institute of Experimental Physics, Slovak Academy of Sciences, 2009) p. 27
102. Garrard T L et al., in *Proc. of the 25th Intern. Cosmic Ray Conf., 30 July – 6 August, 1997, Durban, South Africa* Vol. 1 (Eds M S Potgieter, C Raubenheimer, D J van der Walt) (Transvaal: Potchefstroom Univ., 1997) p. 105
103. Stone E C et al. *Space Sci. Rev.* **86** 1 (1998)
104. Cummings A C, Stone E C *AIP Conf. Proc.* **1516** 97 (2013)
105. Cummings A C, Stone E C, Webber W R *Astrophys. J. Lett.* **287** L99 (1984)
106. McComas D J, Schwadron N A *Geophys. Res. Lett.* **33** L04102 (2006)
107. Kóta J, in *Proc. of the 30th Intern. Cosmic Ray Conf., July 3–11, 2007, Merida, Yucatan, Mexico* Vol. 1 (Eds R Caballero et al.) (Mexico: Univ. Nacional Autónoma de México, 2008) p. 853
108. Jokipii J R, Kóta J *AIP Conf. Proc.* **1039** 390 (2008)
109. Drake J F et al. *Astrophys. J.* **709** 963 (2010)
110. Lazarian A, Opher M *Astrophys. J.* **703** 8 (2009)
111. Fisk L A, Gloeckler G *Adv. Space Res.* **43** 1471 (2009)
112. Fisk L A, Kozlovsky B, Ramaty R *Astrophys. J. Lett.* **190** L35 (1974)
113. Mason G M et al. *AIP Conf. Proc.* **1039** 101 (2008)
114. Mason G M et al. *Astrophys. J.* **678** 1458 (2008)
115. Fisk L A, Lee M A *Astrophys. J.* **237** 620 (1980)
116. Zank G P et al. *Astrophys. J.* **814** 137 (2015)
117. Adhikari L et al. *Astrophys. J.* **873** 72 (2019)
118. Miroshnichenko L I, in *Elektromagnitnye i Plazmennye Protsessy ot Nedr Solntsa do Nedr Zemli* (Electromagnetic and Plasma Processes from the Interior of the Sun to the Interior of the Earth) (Ed. V D Kuznetsov) (Moscow: IZMIRAN, 2015) p. 285
119. Bazilevskaya G A "O proiskhozhdenii solnechnykh kosmicheskikh luchei: Eksperimental'nye dannye" ("On the origin of Solar cosmic rays: Experimental data"), in *34-ya Vseross. Konf. po Kosmicheskim Lucham, Dubna, 15–19 Avgusta 2016* (34th All-Russian Conf. on Cosmic Rays, Dubna, August 15–19, 2016), Review invited talk
120. Bazilevskaya G A *J. Phys. Conf. Ser.* **798** 012034 (2017)
121. Reames D V *Solar Energetic Particles: A Modern Primer on Understanding Sources, Acceleration and Propagation* (Lecture Notes in Physics, Vol. 932) (New York: Springer, 2017) https://doi.org/10.1007/978-3-319-50871-9
122. Miroshnichenko L I *J. Space Weather Space Clim.* **8** A52 (2018)
123. Filippov A T, Chirkov N P, in *Proc. of the 15th Intern. Cosmic Ray Conf., Plovdiv, Bulgaria* Vol. 5 (Sofia: Bulgarian Academy of Sciences, 1977) p. 208
124. Miroshnichenko L I, in *Proc. of the 15th Intern. Cosmic Ray Conf., Plovdiv, Bulgaria* Vol. 5 (Sofia: Bulgarian Academy of Sciences, 1977) p. 214
125. Miroshnichenko L I, in *Problemy Fiziki Solnechnykh Vspyshek. Materialy Ezhegodnogo Seminara Sektsii 'Solntse', 15–18 Dekabrya 1981 g.* (Problems in the Physics of Solar Flares. Materials of the Annual Seminar of the Section "Sun", December 15–18, 1981) (Exec. Ed. A A Korchak) (Moscow: IZMIRAN, 1983) p. 120
126. Miroshnichenko L I, Nymmik R A *Radiation Measurements* **61** 6 (2014)
127. Nymmik R A *Cosmic Res.* **49** 240 (2011); *Kosmicheskie Issled.* **49** 249 (2011)
128. Nymmik R A *Bull. Russ. Acad. Sci. Phys.* **75** 761 (2011); *Izv. Ross. Akad. Nauk. Ser. Fiz.* **75** 810 (2011)
129. Krymskii G F et al. *JETP Lett.* **102** 335 (2015); *Pis'ma Zh. Eksp. Teor. Fiz.* **102** 372 (2015)
130. Band D et al. *Astrophys. J.* **413** 281 (1993)
131. Raukunen O et al. *J. Space Weather Space Clim.* **8** A04 (2018)
132. Bogachev S A, Somov B V *Astron. Lett.* **31** 537 (2005); *Pis'ma Astron. Zh.* **31** 601 (2005)
133. Somov B V *Plasma Astrophysics* Pt. 1 *Fundamental and Practice* (Astrophysics and Space Science Library, Vol. 391) 2nd ed. (New York: Springer, 2013); Somov B V *Plasma Astrophysics* Pt. 2 *Reconnection and Flares* (Astrophysics and Space Science Library, Vol. 392) 2nd ed. (New York: Springer, 2013)
134. Dorman L I, Miroshnichenko L I *Solar Cosmic Rays* (Washington, DC: NASA, 1976); Translated from Russian: *Solnechnye Kosmicheskie Luchi* (Moscow: Nauka, 1968)
135. Schlickeiser R *Cosmic Ray Astrophysics* (Berlin: Springer, 2002)
136. Korchak A A, Syrovatsky S I, in *Proc. 6th Intern. Cosmic Ray Conf., Moscow, USSR, July 6–11, 1959* Vol. 3 (Ed. S I Syrovatsky) (Moscow, 1960) p. 211
137. Ostryakov V M, Kartavykh Yu Yu, Koval'tsov G A *Astron. Lett.* **26** 122 (2000); *Pis'ma Astron. Zh.* **26** 153 (2000)
138. Ostryakov V M, Stovpyuk M F *Solar Phys.* **217** 281 (2003)
139. Kartavykh Y Y et al. *Astrophys. J.* **888** 48 (2020)
140. Tylka A J et al. *Astrophys. J.* **625** 474 (2005)
141. Cliver E W, in *Universal Heliophysical Processes. Proc. of the 257th Symp. of the Intern. Astronomical Union, Ioannina, Greece, September 15 – 19, 2008* (IAU Symp., Vol. 257, Eds N Gopalswamy, D F Webb) (Cambridge: Cambridge Univ. Press, 2009) p. 401
142. Hudson H S, Cliver E W *J. Geophys. Res.* **106** 25199 (2001)
143. Al-Sawad A et al. *Astrophys. Space Sci. Trans.* **8** 1 (2012)
144. Zank G P, Rice W K M, Wu C C *J. Geophys. Res.* **105** 25079 (2000)
145. Ellison D C, Ramaty R *Astrophys. J.* **298** 400 (1985)
146. Miroshnichenko L I, Perez-Peraza J A *Int. J. Mod. Phys. A* **23** 1 (2008)
147. Mewaldt R A et al., in *Proc. of the 30th Intern. Cosmic Ray Conf., July 3–11, 2007, Merida, Yucatán, Mexico* Vol. 1 (Eds R Caballero

et al.) (Mexico: Universidad Nacional Autónoma de México, 2008) p. 107
148. Mewaldt R A et al. *J. Geophys. Res.* **110** A09S18 (2005)
149. Mewaldt R A et al. *AIP Conf. Proc.* **781** 227 (2005)
150. Li G, Zank G P, Rice W K M *J. Geophys. Res.* **110** A06104 (2005)
151. Li C et al. *Astrophys. J.* **770** 34 (2013)
152. Li C, Miroshnichenko L I, Fang C *Res. Astron. Astrophys.* **15** 1036 (2015)
153. Li C, Miroshnichenko L I, Sdobnov V E *Solar Phys.* **291** 975 (2016)
154. Miroshnichenko L I, Li C, Yanke V G *Cosmic Res.* **58** 150 (2020); *Kosmicheskie Issled.* **58** 191 (2020)
155. Miroshnichenko L I, Li C, Yanke V G *Solar Phys.* **295** 102 (2020)
156. Berezhko E G, Taneev S N *Astron. Lett.* **29** 530 (2003); *Pis'ma Astron. Zh.* **29** 601 (2003)
157. Berezhko E G, Taneev S N *Astron. Lett.* **39** 393 (2013); *Pis'ma Astron. Zh.* **39** 443 (2013)
158. Mishev A, Poluianov S, Usoskin I *J. Space Weather Space Clim.* **7** A28 (2017)
159. Poluianov S V et al. *Solar Phys.* **292** 176 (2017)
160. Miroshnichenko L I, De Koning C A, Perez-Enriquez R *Space Sci. Rev.* **91** 615 (2000)
161. Berezhko E G, Krymskii G F *Sov. Phys. Usp.* **31** 27 (1988); *Usp. Fiz. Nauk* **154** 49 (1988)
162. Gopalswamy N et al. *Astrophys. J. Lett.* **765** L30 (2013)
163. Tylka A J, in *Proc. of the 26th Intern. Cosmic Ray Conf., August 17–25, 1999, Salt Lake City, Utah, USA* Vol. 6 (Eds D Kieda, M Salamon, B Dingu) (Salt Lake City, UT, 1999) p. 67
164. Lovell J L, Duldig M L, Humble J E *J. Geophys. Res.* **103** 23733 (1998)
165. Maurchev E A et al. *Bull. Russ. Acad. Sci. Phys.* **85** 277 (2021); *Izv. Ross. Akad. Nauk. Ser. Fiz.* **85** 388 (2021)
166. Reames D V *Solar Phys.* **295** 113 (2020)
167. Reames D V, Ng C K *Astrophys. J.* **504** 1002 (1998)
168. Reames D V *Solar Phys.* **296** 24 (2021)
169. Zank G P et al. *Phys. Plasmas* **8** 4560 (2001)
170. Gaisser T K, Engel R, Resconi E *Cosmic Rays and Particle Physics* 2nd ed. (Cambridge: Cambridge Univ. Press, 2016) https://doi.org/10.1017/CBO9781139192194
171. Wolfendale A, Erlykin A *Astropart. Phys.* **53** 115 (2014)
172. Bykov A M et al. *Space Sci. Rev.* **214** 41 (2018)
173. Anchordoqui L A *Phys. Rep.* **801** 1 (2019)
174. Kachelrieß M, Semikoz D V, INSPIRE HEP. Literature, https://inspirehep.net/literature/1730269
175. Zatsepin V I et al. *Izv. Ross. Akad. Nauk. Ser. Fiz.* **68** 1593 (2004)
176. Panov A D et al. *Bull. Russ. Acad. Sci. Phys.* **73** 564 (2009); *Izv. Ross. Akad. Nauk. Ser. Fiz.* **73** 602 (2009)
177. Zatsepin V I, Panov A D, Sokol'skaya N V, in *31-ya Vserossiiskaya Konf. po Kosmicheskim Lucham, Moscow, MGU, 5–9 Iyulya 2010* (31st All-Russian Conf. on Cosmic Rays, Moscow, Moscow State Univ., July 5–9, 2010) (Moscow: MGU, 2010) PCR-40
178. Chang J et al. *Nature* **456** 362 (2008)
179. Buitink S et al. (LOFAR Collab.) *Nature* **531** 70 (2016)
180. Buitink S et al. (LOFAR Collab.), arXiv:1603.01594
181. Troitsky S V *JETP Lett.* **96** 13 (2012); *Pis'ma Zh. Eksp. Teor. Fiz.* **96** 14 (2012)
182. Fairbairn M, Rashba T, Troitsky S *Phys. Rev. D* **84** 125019 (2011)
183. Kulikov G V, Khristiansen G B *Sov. Phys. JETP* **8** 441 (1959); *Zh. Eksp. Teor. Fiz.* **35** 635 (1958)
184. Bykov A M, Toptygin A M *Izv. Ross. Akad. Nauk. Ser. Fiz.* **59** 162 (1995)
185. Rieger F M, Bosch-Ramon V, Duffy P *Astrophys. Space Sci.* **309** 119 (2007)
186. Lemoine M, Waxman E *J. Cosmol. Astropart. Phys.* (11) 009 (2009)
187. Lemoine M *J. Phys. Conf. Ser.* **409** 012007 (2013)
188. Kichigin G N *Adv. Space Res.* **51** 309 (2013)
189. Kichigin G N *Solnechno-Zemnaya Fiz.* **1** (1) 109 (2015)
190. Vilenkin A, Shellard E P S *Cosmic Strings and other Topological Defects* (Cambridge: Cambridge Univ. Press, 1994)
191. Berezinskii V S, "Kurs videolektsii: "Kosmicheskie luchi vysokikh i sverkhvysokikh energii"' ("Course of video lectures 'Cosmic rays of high and ultrahigh energies"') (2013), https://old.mephi.ru/students/vl/cosmicrays/index.php; https://youtu.be/F1WRPsu1QU4
192. Parker E N *Astrophys. J.* **128** 664 (1958)
193. Cowsik R, Lee M A *Proc. R. Soc. Lond. A* **383** 409 (1982)
194. Schneider P, Bogdan T J *Astrophys. J.* **347** 496 (1989)
195. Krymskii G F *Sov. Phys. Dokl.* **22** 327 (1977); *Dokl. Akad. Nauk SSSR* **234** 1306 (1977)
196. Axford W I, Leer E, Skadron G, in *Proc. of the 15th Intern. Cosmic Ray Conf., Plovdiv, Bulgaria* Vol. 11 (Sofia: Bulgarian Academy of Sciences, 1977) p. 132
197. Bell A R *Mon. Not. R. Astron. Soc.* **182** 147 (1978)
198. Blandford R D, Ostriker J P *Astrophys. J. Lett.* **221** L29 (1978)
199. Berezhko E G *JETP Lett.* **33** 399 (1981); *Pis'ma Zh. Eksp. Teor. Fiz.* **33** 416 (1981)
200. Berezhko E G, Krymskii G F *Sov. Astron. Lett.* **7** 352 (1981); *Pis'ma Astron. Zh.* **7** 636 (1981)
201. Berezhko E G, Krymskii G F *Sov. Phys. Usp.* **31** 27 (1988); *Usp. Fiz. Nauk* **154** 49 (1988)
202. Fölk G *Izv. Akad. Nauk SSSR. Ser. Fiz.* **45** 1122 (1981)
203. Jones F C *Astrophys. J. Suppl.* **90** 561 (1994)
204. Miroshnichenko L I *Solar Phys.* **156** 119 (1995)
205. Bykov A M, Toptygin I N *Phys. Usp.* **50** 141 (2007); *Usp. Fiz. Nauk* **177** 149 (2007)
206. Dorman L *Adv. Space Res.* **64** 2418 (2019)
207. Stozhkov Yu I *Bull. Russ. Acad. Sci. Phys.* **75** 323 (2011); *Izv. Ross. Akad. Nauk SSSR Ser. Fiz.* **75** 352 (2011)
208. Adriani O et al. (PAMELA Collab.) *Science* **332** 69 (2011)
209. Dreicer H *Phys. Rev.* **115** 238 (1959)
210. Shibata K et al. *Publ. Astron. Soc. Jpn.* **65** (3) 49 (2013)
211. Shibayama T et al. *Astrophys. J. Suppl. Ser.* **209** 5 (2013)
212. Kalmykov N N, Kulikov G V, in *Akademik Sergei Nikolaevich Vernov. K 100-letiyu so Dnya Rozhdeniya* (Academician Sergei Nikolaevich Vernov. To the 100th Anniversary of the Birth) (Moscow: Izd. MGU, 2010) p. 72
213. Troitsky S V et al., in *Searching for the Origins of Cosmic Rays, June 15–18, 2009, Symp., Trondheim, Norway, 2009*; http://web.phys.ntnu.no/~mika/programme.html
214. Troitsky S V *Phys. Usp.* **55** 72 (2012); *Usp. Fiz. Nauk* **182** 77 (2012)
215. Abbasi R U et al. (HiRes Collab.) *Astrophys. J.* **636** 680 (2006)
216. Kovalev V A *Slozhnye Sistemy* **3** (16) 50 (2015)
217. Samarskii A A et al. *Blow-up in Quasilinear Parabolic Equations* (De Gruyter Expositions in Mathematics, Vol. 19) (Berlin: De Gruyter, 1995); Translated from Russian: *Rezhimy s Obostreniem v Zadachakh dlya Kvazilineinykh Parabolicheskikh Uravnenii* (Moscow: Nauka, 1987)
218. Somov B V, Kosugi T *Astrophys. J.* **485** 859 (1997)
219. Kovalev V A, Somov B V *Astron. Lett.* **29** 409 (2003); *Pis'ma Astron. Zh.* **29** 465 (2003)
220. Miroshnichenko L I *Radiation Hazard in Space* (Dordrecht: Kluwer Acad. Publ., 2003)
221. Miroshnichenko L I *Fizika Solntsa i Solnechno-Zemnykh Svyazei* (Moscow: Univ. Kniga, 2011)
222. Katsouleas T *Nature* **431** 515 (2004)
223. Kropotina Yu A et al. *Tech. Phys.* **61** 517 (2016); *Zh. Tekh. Fiz.* **86** (4) 40 (2016)
224. Caprioli D, Yi D T, Spitkovsky A *Phys. Rev. Lett.* **119** 171101 (2017)
225. Kropotina Yu A et al. *Tech. Phys.* **60** 231 (2015); *Zh. Tekh. Fiz.* **85** (2) 73 (2015)
226. Kropotina Yu A et al. *Tech. Phys.* **65** 14 (2020); *Zh. Tekh. Fiz.* **90** (1) 18 (2020)
227. Kropotina Yu A "Gibridnoe modelirovanie besstolknovitel'nykh udarnykh voln v mnogokomponentnoi plazme ostatkov sverkhnovykh, skoplenie galaktik i solnechnogo vetra" ("Hybrid simulation of collisionless shock waves in multicomponent plasma of supernova remnants, galaxy clusters, and Solar wind"), Abstract Ph.D. Thesis (Phys.-Math. Sciences) (St. Petersburg: Ioffe Inst., 2021)
228. Li T M et al. *Astrophys. J.* **922** 50 (2021)
229. Matthews S A et al. *Exp. Astron.* **33** 237 (2012)
230. Cocconi D, in *Proc. of the 6th Intern. Cosmic Ray Conf., July 6–11, 1959, Moscow, USSR* Vol. 3 (Ed. S I Syrovatsky) (Moscow, 1960) p. 256
231. Balega Yu Yu et al. *Phys. Usp.* **64** 317 (2021); *Usp. Fiz. Nauk* **191** 331 (2021)